J Sci Comput (2013) 54:121–144
DOI 10.1007/s10915-012-9608-5

Numerical Study of the Plasma-Lorentz Model in Metamaterials

Jichun Li · Yunqing Huang · Wei Yang

Received: 17 February 2012 / Revised: 3 May 2012 / Accepted: 13 May 2012 /
Published online: 26 May 2012

Abstract Since 2000, the study of metamaterial has been a very hot topic due to its potential applications in many areas such as design of invisibility cloak and sub-wavelength imaging. Although several metamaterial models are often used by physicists and engineers, the study of their mathematical properties has lagged behind. In this paper, we initiate our investigation in the plasma-Lorentz model. More specifically, we first discuss the well-posedness of this model, then develop two fully-discrete finite element methods for solving it. Detailed stability and error analysis are carried out, and 3-D numerical results justifying our theoretical analysis are presented.

Keywords Maxwell's equations · Metamaterial · Plasma-Lorentz model · Finite element method

1 Introduction

In 2000, Smith et al. [42] successfully constructed a composite medium with simultaneously negative electric permittivity and magnetic permeability. An electromagnetic material with this property is usually called metamaterial. Later on, the first experimental demonstration of the negative refraction index was carried out for the metamaterial [40]. Since

J. Li (✉)
Department of Mathematical Sciences, University of Nevada Las Vegas, Las Vegas, NV 89154-4020, USA
e-mail: jichun@unlv.nevada.edu

Y. Huang · W. Yang
Hunan Key Laboratory for Computation and Simulation in Science and Engineering, Xiangtan University, Xiangtan 411105, China

Y. Huang
e-mail: huangyq@xtu.edu.cn

W. Yang
e-mail: yangweixtu@126.com

2000, there has been a tremendous growing interest in the study of metamaterial and its potential applications in areas ranging from electronics, telecommunications to sensing, radar technology, sub-wavelength imaging, data storage, and design of invisibility cloak. More details on metamaterials can be found in some recent monographs such as [9, 12, 17, 29] and references cited therein.

Though numerical simulations for metamaterials are often used by engineers and physicists, they mainly use the classic finite-difference time-domain (FDTD) method [45]. However, it is known that the FDTD method has a big disadvantage for solving problems with complex geometries. Hence it would be quite interesting and useful to develop efficient and robust finite element methods (FEMs) for modeling metamaterials.

The metamaterial models can be described by the Maxwell's equations augmented with some constitutive equations. Hence the study of metamaterial models is more complicated than the standard Maxwell's equations in vacuum. Though there exist many excellent work for Maxwell's equations in vacuum (e.g., papers [2, 4, 6–8, 14, 16, 19, 20, 22, 27, 34, 35], books [10, 18, 30] and references cited therein) and in dispersive media (e.g., [1, 5, 11, 26, 28, 36–38, 44, 46]), to our best knowledge, there are not much work devoted to the development and analysis of FEMs for the Maxwell's equations when metamaterials are involved [13]. In recent years, we made some initial effort [21, 23–25] in developing and analyzing some FEMs for time-domain Maxwell's equations involving metamaterials. However, our previous papers were restricted to metamaterial models whose permittivity and permeability are given by the same type constitutive relations such as the so-called Drude model or Lorentz model.

In this paper, we will investigate another type metamaterial model used by engineers and physicists, in which the permittivity is described by a plasma model, while the permeability is described by the Lorentz model. To be specific, we denote this model as the plasma-Lorentz model, which has not been studied before from the mathematics point view, though this model has been used by engineers and physicists [3, 32, 33, 39, 41]. Here we first study its well-posedness, then develop two fully-discrete finite element methods for solving this model. Detailed stability analysis, error estimates and numerical results supporting the analysis are carried out.

In this paper, $C > 0$ denotes a generic constant, which is independent of the finite element mesh size h and time step size τ. Let $(H^\alpha(\Omega))^3$ be the standard Sobolev space equipped with the norm $\|\cdot\|_\alpha$ and semi-norm $\|\cdot\|_\alpha$. Specifically, $\|\cdot\|_0$ will mean the $(L^2(\Omega))^3$-norm. We also introduce some common notation [30]:

$$H(\mathrm{curl};\Omega) = \left\{\boldsymbol{v} \in \left(L^2(\Omega)\right)^3;\ \nabla \times \boldsymbol{v} \in \left(L^2(\Omega)\right)^3\right\},$$

$$H_0(\mathrm{curl};\Omega) = \left\{\boldsymbol{v} \in H(\mathrm{curl};\Omega);\ \mathbf{n} \times \boldsymbol{v} = 0 \text{ on } \partial\Omega\right\},$$

$$H^\alpha(\mathrm{curl};\Omega) = \left\{\boldsymbol{v} \in \left(H^\alpha(\Omega)\right)^3;\ \nabla \times \boldsymbol{v} \in \left(H^\alpha(\Omega)\right)^3\right\},$$

where $\alpha \geq 0$ is a real number, and Ω is a bounded Lipschitz polyhedral domain in $\mathcal{R}^3$ with connected boundary $\partial\Omega$. We equip $H(\mathrm{curl};\Omega)$ with norm $\|\boldsymbol{v}\|_{0,\mathrm{curl}} = (\|\boldsymbol{v}\|_0^2 + \|\mathrm{curl}\ \boldsymbol{v}\|_0^2)^{1/2}$, and $H^\alpha(\mathrm{curl};\Omega)$ with norm $\|\boldsymbol{v}\|_{\alpha,\mathrm{curl}} = (\|\boldsymbol{v}\|_\alpha^2 + \|\mathrm{curl}\ \boldsymbol{v}\|_\alpha^2)^{1/2}$. For clarity, we introduce the vector notation

$$\boldsymbol{L}^2(\Omega) = \left(L^2(\Omega)\right)^3, \qquad \boldsymbol{H}^\alpha(\Omega) = \left(H^\alpha(\Omega)\right)^3, \qquad \boldsymbol{H}^\alpha(\mathrm{curl};\Omega) = \left(H^\alpha(\mathrm{curl};\Omega)\right)^3.$$

The rest of the paper is organized as follows. In Sect. 2, we present the governing equations for the plasma-Lorentz metamaterial model. In Sect. 3, we develop two fully-discrete schemes, and prove the corresponding stability analysis and error estimates. Then in Sect. 4, we present some numerical results justifying our theoretical analysis. Finally, we conclude our paper in Sect. 5.

2 The Governing Equations

To simulate electromagnetic wave propagation, we have to solve the general Maxwell's equations

$$\nabla \times \boldsymbol{E} = -\frac{\partial \boldsymbol{B}}{\partial t}, \qquad \nabla \times \boldsymbol{H} = \frac{\partial \boldsymbol{D}}{\partial t}, \tag{2.1}$$

where $\boldsymbol{E}(\boldsymbol{x},t)$ and $\boldsymbol{H}(\boldsymbol{x},t)$ are the electric and magnetic fields, $\boldsymbol{D}(\boldsymbol{x},t)$ and $\boldsymbol{B}(\boldsymbol{x},t)$ are the corresponding electric and magnetic flux densities. In a general medium, $\boldsymbol{D}$ and $\boldsymbol{B}$ are related to $\boldsymbol{E}$ and $\boldsymbol{H}$ through the constitutive relations

$$\boldsymbol{D} = \epsilon_0 \boldsymbol{E} + \boldsymbol{P} \equiv \epsilon \boldsymbol{E}, \qquad \boldsymbol{B} = \mu_0 \boldsymbol{H} + \boldsymbol{M} \equiv \mu \boldsymbol{H}, \tag{2.2}$$

where ϵ_0 and μ_0 are the permittivity and permeability in free space, respectively, and $\boldsymbol{P}$ and $\boldsymbol{M}$ are polarization and magnetization, respectively. Moreover, ϵ and μ are the permittivity and permeability of the underlying medium, respectively.

The permittivity can be described by the cold electron plasma model [32, 33]:

$$\epsilon(\omega) = \epsilon_0 \left(1 - \frac{\omega_p^2}{\omega(\omega + j\nu)}\right), \tag{2.3}$$

where ω is the excitation angular frequency, $\omega_p > 0$ is the effective plasma frequency, $\nu \geq 0$ is the loss parameter, and $j = \sqrt{-1}$ is the imaginary unit. On the other hand, the permeability can be described by the Lorentz model [39, 41]:

$$\mu(\omega) = \mu_0 \left(1 - \frac{F\omega_0^2}{\omega^2 + j\gamma\omega - \omega_0^2}\right), \tag{2.4}$$

where $\omega_0 > 0$ is the resonant frequency, $\gamma \geq 0$ is the loss parameter, and $F \in (0, 1)$ is a parameter depending on the geometry of the unit cell of the metamaterial.

Using a time-harmonic variation of $\exp(j\omega t)$, and substituting (2.3) and (2.4) into (2.2), respectively, we obtain the time-domain equation for the polarization:

$$\frac{\partial^2 \boldsymbol{P}}{\partial t^2} + \nu \frac{\partial \boldsymbol{P}}{\partial t} = \epsilon_0 \omega_p^2 \boldsymbol{E}, \tag{2.5}$$

and the equation for the magnetization:

$$\frac{\partial^2 \boldsymbol{M}}{\partial t^2} + \gamma \frac{\partial \boldsymbol{M}}{\partial t} + \omega_0^2 \boldsymbol{M} = \mu_0 F \omega_0^2 \boldsymbol{H}. \tag{2.6}$$

To facility the mathematical study of the model, by introducing the induced electric current $\boldsymbol{J} = \frac{\partial \boldsymbol{P}}{\partial t}$ and magnetic current $\boldsymbol{K} = \frac{\partial \boldsymbol{M}}{\partial t}$, we can write the time domain governing equations for the plasma-Lorentz model as following:

$$\epsilon_0 \frac{\partial \boldsymbol{E}}{\partial t} = \nabla \times \boldsymbol{H} - \boldsymbol{J}, \tag{2.7}$$

$$\mu_0 \frac{\partial \boldsymbol{H}}{\partial t} = -\nabla \times \boldsymbol{E} - \boldsymbol{K}, \tag{2.8}$$

$$\frac{1}{\mu_0 \omega_0^2 F} \frac{\partial \boldsymbol{K}}{\partial t} + \frac{\gamma}{\mu_0 \omega_0^2 F} \boldsymbol{K} + \frac{1}{\mu_0 F} \boldsymbol{M} = \boldsymbol{H}, \tag{2.9}$$

$$\frac{1}{\mu_0 F} \frac{\partial \boldsymbol{M}}{\partial t} = \frac{1}{\mu_0 F} \boldsymbol{K}, \tag{2.10}$$

$$\frac{1}{\epsilon_0 \omega_p^2} \frac{\partial \boldsymbol{J}}{\partial t} + \frac{\nu}{\epsilon_0 \omega_p^2} \boldsymbol{J} = \boldsymbol{E}. \tag{2.11}$$

To complete the model problem (2.7)–(2.11), we assume that the boundary of Ω is perfect conducting so that

$$\boldsymbol{n} \times \boldsymbol{E} = \boldsymbol{0} \quad \text{on } \partial\Omega, \tag{2.12}$$

where $\boldsymbol{n}$ is the unit outward normal to $\partial\Omega$. Furthermore, we assume that the initial conditions are

$$\boldsymbol{E}(\mathbf{x}, 0) = \boldsymbol{E}_0(\mathbf{x}), \qquad \boldsymbol{H}(\mathbf{x}, 0) = \boldsymbol{H}_0(\mathbf{x}), \tag{2.13}$$

$$\boldsymbol{K}(\mathbf{x}, 0) = \boldsymbol{K}_0(\mathbf{x}), \qquad \boldsymbol{M}(\boldsymbol{x}, 0) = \boldsymbol{M}_0(\mathbf{x}), \qquad \boldsymbol{J}(\boldsymbol{x}, 0) = \boldsymbol{J}_0(\mathbf{x}), \tag{2.14}$$

where $\boldsymbol{E}_0$, $\boldsymbol{H}_0$, $\boldsymbol{K}_0$, $\boldsymbol{M}_0$ and $\boldsymbol{J}_0$ are some given functions.

First, we have the following stability for our model problem (2.7)–(2.11).

Lemma 2.1 *For the solution* $(\boldsymbol{E}, \boldsymbol{H}, \boldsymbol{K}, \boldsymbol{M}, \boldsymbol{J})$ *of the model problem* (2.7)–(2.11) *with boundary condition* (2.12) *and initial conditions* (2.13)–(2.14), *the following stability holds true*:

$$\epsilon_0 \|\boldsymbol{E}(t)\|_0^2 + \mu_0 \|\boldsymbol{H}(t)\|_0^2 + \frac{1}{\mu_0 \omega_0^2 F} \|\boldsymbol{K}(t)\|_0^2 + \frac{1}{\mu_0 F} \|\boldsymbol{M}(t)\|_0^2 + \frac{1}{\epsilon_0 \omega_p^2} \|\boldsymbol{J}(t)\|_0^2$$
$$\leq \epsilon_0 \|\boldsymbol{E}_0\|_0^2 + \mu_0 \|\boldsymbol{H}_0\|_0^2 + \frac{1}{\mu_0 \omega_0^2 F} \|\boldsymbol{K}_0\|_0^2 + \frac{1}{\mu_0 F} \|\boldsymbol{M}_0\|_0^2 + \frac{1}{\epsilon_0 \omega_p^2} \|\boldsymbol{J}_0\|_0^2. \tag{2.15}$$

Proof Note that the problem (2.7)–(2.11) can be rewritten as

$$\frac{\partial}{\partial t} \mathcal{A} \boldsymbol{u}(t) = (\mathcal{B} + \mathcal{C}) \boldsymbol{u}(t), \tag{2.16}$$

where we denote $\boldsymbol{u}(t) = (\boldsymbol{E}, \boldsymbol{H}, \boldsymbol{K}, \boldsymbol{M}, \boldsymbol{J})'$, operators

$$\mathcal{A} = \operatorname{diag}\left(\epsilon_0 I, \mu_0 I, \frac{1}{\mu_0 \omega_0^2 F} I, \frac{1}{\mu_0 F} I, \frac{1}{\epsilon_0 \omega_p^2} I\right),$$

$$\mathcal{C} = \operatorname{diag}\left(0, 0, -\frac{\gamma}{\mu_0 \omega_0^2 F} I, 0, -\frac{\nu}{\epsilon_0 \omega_p^2} I\right),$$

and

$$\mathcal{B}=\begin{pmatrix} 0 & \nabla\times & 0 & 0 & -I \\ -\nabla\times & 0 & -I & 0 & 0 \\ 0 & I & 0 & -\frac{1}{\mu_0 F}I & 0 \\ 0 & 0 & \frac{1}{\mu_0 F}I & 0 & 0 \\ I & 0 & 0 & 0 & 0 \end{pmatrix},$$

here I denotes a 3×3 identity matrix. Note that the operator $\mathcal{B}$ is anti-symmetric.

To prove the stability, multiplying (2.16) by $\boldsymbol{u}'$, then integrating over Ω, and using the property $\boldsymbol{u}'\mathcal{B}\boldsymbol{u}=0$, we obtain

$$\frac{d}{dt}\big(\boldsymbol{u}'\mathcal{A}\boldsymbol{u}\big)=\boldsymbol{u}'\mathcal{C}\boldsymbol{u}\le 0,$$

integrating which with respect to t leads to the stability (2.15). □

Remark 2.1 The stability (2.15) can be proved in a direct way. Multiplying (2.7)–(2.11) by $\boldsymbol{E}, \boldsymbol{H}, \boldsymbol{K}, \boldsymbol{M}, \boldsymbol{J}$ and integrating over Ω, then adding the resultants together, we obtain

$$\frac{1}{2}\frac{d}{dt}\left[\epsilon_0\|\boldsymbol{E}(t)\|_0^2+\mu_0\|\boldsymbol{H}(t)\|_0^2+\frac{1}{\mu_0\omega_0^2F}\|\boldsymbol{K}(t)\|_0^2+\frac{1}{\mu_0 F}\|\boldsymbol{M}(t)\|_0^2+\frac{1}{\epsilon_0\omega_p^2}\|\boldsymbol{J}(t)\|_0^2\right]$$
$$+\frac{\nu}{\epsilon_0\omega_p^2}\|\boldsymbol{J}(t)\|_0^2+\frac{\gamma}{\mu_0\omega_0^2F}\|\boldsymbol{K}(t)\|_0^2=0,$$

integrating which from 0 to t leads to (2.15). This is the main reason why we write the last three governing equations (2.9)–(2.11) in this way.

Now, let us prove the existence for our model problem (2.7)–(2.11).

Lemma 2.2 *The problem* (2.7)–(2.11) *has a unique solution* $(\boldsymbol{E},\boldsymbol{H})$ *in* $H(\mathrm{curl};\Omega)\oplus H(\mathrm{curl};\Omega)$.

Proof From ordinary differential equation theory, we can prove that the solutions of (2.5) and (2.6) with zero initial conditions can be expressed as

$$\boldsymbol{P}(\boldsymbol{x},t)=\frac{\epsilon_0\omega_p^2}{\nu}\int_0^t\big(1-e^{-\nu(t-s)}\big)\boldsymbol{E}(\boldsymbol{x},s)ds, \tag{2.17}$$

and

$$\boldsymbol{M}(\boldsymbol{x},t)=\mu_0F\omega_0^2\int_0^t g(t-s)\boldsymbol{H}(\boldsymbol{x},s)ds, \tag{2.18}$$

respectively. Here the kernel $g(t)=\frac{1}{\alpha}e^{-\frac{\gamma}{2}t}\sin(\alpha t)$, where $\alpha=\sqrt{\omega_0^2-(\frac{\gamma}{2})^2}$.

Using the definition $\boldsymbol{J}=\frac{\partial \boldsymbol{P}}{\partial t}$ and $\boldsymbol{K}=\frac{\partial \boldsymbol{M}}{\partial t}$, then substituting (2.17) and (2.18) into (2.7) and (2.8), respectively, we can rewrite (2.7) and (2.8) as follows:

$$\frac{d}{dt}(A\mathcal{E}+\mathcal{K}*\mathcal{E})=L\mathcal{E}+\mathcal{F}, \tag{2.19}$$

where we denote $\mathcal{E} = (\boldsymbol{E}, \boldsymbol{H})$, $*$ for the convolution product, $\mathcal{F}$ for source terms obtained by transforming a problem with non-zero initial conditions to a problem with zero initial conditions, and operators

$$A = \begin{pmatrix} \epsilon_0 I_3 & 0_3 \\ 0_3 & \mu_0 I_3 \end{pmatrix}, \qquad K = \begin{pmatrix} \epsilon_1 I_3 & 0_3 \\ 0_3 & \mu_1 I_3 \end{pmatrix}, \qquad L = \begin{pmatrix} 0_3 & \nabla\times \\ -\nabla\times & 0_3 \end{pmatrix}.$$

In the above, I_3 is the 3×3 unit matrix, 0_3 is the zero matrix, $\epsilon_1 = \frac{\epsilon_0 \omega_p^2}{\nu}(u(t) - e^{-\nu t})$ and $\mu_1 = \mu_0 F \omega_0^2 g(t)$. Here $u(t)$ denotes the unit step function.

Hence our problem (2.19) is a special case of Problem I of [15], whose existence and uniqueness is guaranteed by Theorem 3.1 of [15]. □

Finally, we can prove that the Gauss's Law holds true for our model.

Lemma 2.3 *Assume that the initial fields are divergence free*:

$$\nabla \cdot (\epsilon_0 \boldsymbol{E}_0) = 0, \qquad \nabla \cdot (\mu_0 \boldsymbol{H}_0) = 0, \qquad \nabla \cdot \boldsymbol{K}_0 = 0, \qquad \nabla \cdot \boldsymbol{M}_0 = 0, \qquad \nabla \cdot \boldsymbol{J}_0 = 0,$$

then for any time $t > 0$, *the fields are still divergence free*, *i.e.*, *we have*

$$\nabla \cdot \big(\epsilon_0 \boldsymbol{E}(t)\big) = 0, \qquad \nabla \cdot \big(\mu_0 \boldsymbol{H}(t)\big) = 0, \qquad \nabla \cdot \boldsymbol{K}(t) = 0,$$
$$\nabla \cdot \boldsymbol{M}(t) = 0, \qquad \nabla \cdot \boldsymbol{J}(t) = 0.$$

Proof Taking the divergence of (2.7), we have

$$\frac{\partial}{\partial t}\big(\nabla \cdot (\epsilon_0 \boldsymbol{E})\big) + \nabla \cdot \boldsymbol{J} = 0. \tag{2.20}$$

Similarly, taking the divergence of (2.11), we have

$$\frac{\partial}{\partial t}(\nabla \cdot \boldsymbol{J}) + \nu \nabla \cdot \boldsymbol{J} = \epsilon_0 \omega_p^2 \nabla \cdot \boldsymbol{E}. \tag{2.21}$$

Substituting (2.20) into (2.21), we have

$$\frac{\partial^2}{\partial t^2}(\nabla \cdot \epsilon_0 \boldsymbol{E}) + \nu \frac{\partial}{\partial t}(\nabla \cdot \epsilon_0 \boldsymbol{E}) + \omega_p^2 (\nabla \cdot \epsilon_0 \boldsymbol{E}) = 0. \tag{2.22}$$

By the assumed initial conditions and (2.20), we have initial conditions for $\nabla \cdot \epsilon_0 \boldsymbol{E}$:

$$\nabla \cdot \epsilon_0 \boldsymbol{E}(0) = 0, \qquad \frac{\partial}{\partial t}(\nabla \cdot \epsilon_0 \boldsymbol{E})(0) = -\nabla \cdot \boldsymbol{J}(0) = 0. \tag{2.23}$$

It is easy to see that the ordinary differential equation (2.22) with initial conditions (2.23) only has zero solution, i.e., $\nabla \cdot \epsilon_0 \boldsymbol{E}(t) \equiv 0$.

Other divergence free conditions can be proved similarly. □

3 Fully-Discrete Schemes

In this section, we will develop two fully-discrete finite element methods for solving (2.7)–(2.11). We assume that the domain Ω is partitioned by a family of regular tetrahedral (or cubic) meshes T^h with maximum mesh size h. Depending upon the regularity of the solution of (2.7)–(2.11), we can use a proper order Raviart-Thomas-Nédélec (RTN) mixed finite element space ([30, 31]): For any $l \geq 1$, on a tetrahedral element, we can choose

$$\boldsymbol{U}_h = \left\{\boldsymbol{u}_h \in H(\mathrm{div};\Omega) : \boldsymbol{u}_h|_K \in (p_{l-1})^3 \oplus \tilde{p}_{l-1}\boldsymbol{x},\ \forall K \in T^h\right\},$$
$$\boldsymbol{V}_h = \left\{\boldsymbol{v}_h \in H(\mathrm{curl};\Omega) : \boldsymbol{v}_h|_K \in (p_{l-1})^3 \oplus S_l,\ \forall K \in T^h\right\},\ S_l = \left\{\vec{p} \in (\tilde{p}_l)^3,\ \boldsymbol{x}\cdot\vec{p} = 0\right\},$$

while on a cubic element we choose

$$\boldsymbol{U}_h = \left\{\boldsymbol{u}_h \in H(\mathrm{div};\Omega) : \boldsymbol{u}_h|_K \in Q_{l,l-1,l-1} \times Q_{l-1,l,l-1} \times Q_{l-1,l-1,l},\ \forall K \in T^h\right\},$$
$$\boldsymbol{V}_h = \left\{\boldsymbol{v}_h \in H(\mathrm{curl};\Omega) : \boldsymbol{v}_h|_K \in Q_{l-1,l,l} \times Q_{l,l-1,l} \times Q_{l,l,l-1},\ \forall K \in T^h\right\}.$$

Here $\tilde{p}_k$ denotes the space of homogeneous polynomials of degree k, and $Q_{i,j,k}$ denotes the space of polynomials whose degrees are less than or equal to i, j, k in variables x, y, z, respectively. To impose the boundary condition (2.12), we denote $\boldsymbol{V}_h^0 = \{\boldsymbol{v} \in \boldsymbol{V}_h : \boldsymbol{v} \times \boldsymbol{n} = 0$ on $\partial\Omega\}$. It is easy to see that

$$\nabla \times \boldsymbol{V}_h \subset \boldsymbol{U}_h. \tag{3.1}$$

To carry out the error analysis below, we need to define two operators. The first one is the standard $\boldsymbol{L}^2$-projection operator P_h: For any $\boldsymbol{H} \in \boldsymbol{L}^2(\Omega)$, $P_h\boldsymbol{H} \in \mathbf{U}_h$ satisfies

$$(P_h\boldsymbol{H} - \boldsymbol{H}, \boldsymbol{\psi}_h) = 0, \quad \forall \boldsymbol{\psi}_h \in \mathbf{U}_h.$$

Another one is the standard Nédélec interpolation operator Π_h mapped from $H(\mathrm{curl};\Omega)$ to $\mathbf{V}_h$. It is known that Π_h satisfies the following interpolation error estimate [30, 31]:

$$\|\boldsymbol{E} - \Pi_h\boldsymbol{E}\|_0 + \left\|\nabla \times (\boldsymbol{E} - \Pi_h\boldsymbol{E})\right\|_0 \leq Ch^l\|\boldsymbol{E}\|_{l,\mathrm{curl}}, \quad \forall \boldsymbol{E} \in H^l(\mathrm{curl};\Omega),\ 1 \leq l, \tag{3.2}$$

and P_h has the projection error estimate:

$$\|\boldsymbol{H} - P_h\boldsymbol{H}\|_0 \leq Ch^l\|\boldsymbol{H}\|_l, \quad \forall \boldsymbol{H} \in H^l(\Omega),\ 0 \leq l. \tag{3.3}$$

To define a fully discrete scheme, we divide the time interval $(0, T)$ into N uniform subintervals by points $0 = t_0 < t_1 < \cdots < t_N = T$, where $t_k = k\tau$, $\tau = T/N$, and denote the k-th subinterval by $I_k = [t_{k-1}, t_k]$. Moreover, we define $\boldsymbol{u}^k = \boldsymbol{u}(\cdot, k\tau)$ for $0 \leq k \leq N$, and the notation:

$$\delta_\tau\boldsymbol{u}^k = \left(\boldsymbol{u}^k - \boldsymbol{u}^{k-1}\right)/\tau, \qquad \overline{\boldsymbol{u}}^k = \frac{1}{2}\left(\boldsymbol{u}^k + \boldsymbol{u}^{k-1}\right).$$

3.1 The Crank-Nicolson Scheme

We start with a Crank-Nicolson type scheme for solving (2.7)–(2.11): For $k = 1, 2, \ldots, N$, find $\boldsymbol{E}_h^k \in \boldsymbol{V}_h^0$, $\boldsymbol{J}_h^k \in \boldsymbol{V}_h$, $\boldsymbol{H}_h^k, \boldsymbol{K}_h^k, \boldsymbol{M}_h^k \in \boldsymbol{U}_h$ such that

$$\epsilon_0\left(\delta_\tau\boldsymbol{E}_h^k, \boldsymbol{\phi}_h\right) - \left(\overline{\boldsymbol{H}}_h^k, \nabla \times \boldsymbol{\phi}_h\right) + \left(\overline{\boldsymbol{J}}_h^k, \boldsymbol{\phi}_h\right) = 0, \tag{3.4}$$

$$\mu_0\left(\delta_\tau\boldsymbol{H}_h^k, \boldsymbol{\psi}_h\right) + \left(\nabla \times \overline{\boldsymbol{E}}_h^k, \boldsymbol{\psi}_h\right) + \left(\overline{\boldsymbol{K}}_h^k, \boldsymbol{\psi}_h\right) = 0, \tag{3.5}$$

$$\frac{1}{\mu_0\omega_0^2F}\left(\delta_\tau\boldsymbol{K}_h^k, \tilde{\boldsymbol{\psi}}_{1h}\right) + \frac{\gamma}{\mu_0\omega_0^2F}\left(\overline{\boldsymbol{K}}_h^k, \tilde{\boldsymbol{\psi}}_{1h}\right) + \frac{1}{\mu_0F}\left(\overline{\boldsymbol{M}}_h^k, \tilde{\boldsymbol{\psi}}_{1h}\right) = \left(\overline{\boldsymbol{H}}_h^k, \tilde{\boldsymbol{\psi}}_{1h}\right), \tag{3.6}$$

$$\frac{1}{\mu_0 F}\big(\delta_\tau \boldsymbol{M}_h^k, \tilde{\boldsymbol{\psi}}_{2h}\big) = \frac{1}{\mu_0 F}\big(\overline{\boldsymbol{K}}_h^k, \tilde{\boldsymbol{\psi}}_{2h}\big), \tag{3.7}$$

$$\frac{1}{\epsilon_0\omega_p^2}\big(\delta_\tau \boldsymbol{J}_h^k, \tilde{\boldsymbol{\phi}}_h\big) + \frac{\nu}{\epsilon_0\omega_p^2}\big(\overline{\boldsymbol{J}}_h^k, \tilde{\boldsymbol{\phi}}_h\big) = \big(\overline{\boldsymbol{E}}_h^k, \tilde{\boldsymbol{\phi}}_h\big), \tag{3.8}$$

hold true for any $\boldsymbol{\phi}_h \in \boldsymbol{V}_h^0, \boldsymbol{\psi}_h, \tilde{\boldsymbol{\psi}}_{1h}, \tilde{\boldsymbol{\psi}}_{2h} \in \boldsymbol{U}_h, \tilde{\boldsymbol{\phi}}_h \in \boldsymbol{V}_h$, and are subject to the initial approximations

$$\boldsymbol{E}_h^0(\boldsymbol{x}) = \Pi_h \boldsymbol{E}_0(\boldsymbol{x}), \qquad \boldsymbol{H}_h^0(\boldsymbol{x}) = P_h \boldsymbol{H}_0(\boldsymbol{x}),$$
$$\boldsymbol{K}_h^0(\boldsymbol{x}) = P_h \boldsymbol{K}_0(\boldsymbol{x}), \qquad \boldsymbol{M}_h^0(\boldsymbol{x}) = P_h \boldsymbol{M}_0(\boldsymbol{x}), \qquad \boldsymbol{J}_h^0(\boldsymbol{x}) = \Pi_h \boldsymbol{J}_0(\boldsymbol{x}).$$

First, we can show that our scheme (3.4)–(3.8) satisfies a discrete stability, which has exactly the same form as the continuous case proved in Lemma 2.1.

Lemma 3.1 *For any $k \ge 1$, we have*

$$\begin{aligned}
&\epsilon_0\big\|\boldsymbol{E}_h^k\big\|_0^2 + \mu_0\big\|\boldsymbol{H}_h^k\big\|_0^2 + \frac{1}{\epsilon_0\omega_p^2}\big\|\boldsymbol{J}_h^k\big\|_0^2 + \frac{1}{\mu_0\omega_0^2 F}\big\|\boldsymbol{K}_h^k\big\|_0^2 + \frac{1}{\mu_0 F}\big\|\boldsymbol{M}_h^k\big\|_0^2 \\
&\quad\le \epsilon_0\big\|\boldsymbol{E}_h^0\big\|_0^2 + \mu_0\big\|\boldsymbol{H}_h^0\big\|_0^2 + \frac{1}{\epsilon_0\omega_p^2}\big\|\boldsymbol{J}_h^0\big\|_0^2 + \frac{1}{\mu_0\omega_0^2 F}\big\|\boldsymbol{K}_h^0\big\|_0^2 + \frac{1}{\mu_0 F}\big\|\boldsymbol{M}_h^0\big\|_0^2.
\end{aligned} \tag{3.9}$$

Proof Choosing $\boldsymbol{\phi}_h = \tau\overline{\boldsymbol{E}}_h^k, \boldsymbol{\psi}_h = \tau\overline{\boldsymbol{H}}_h^k, \tilde{\boldsymbol{\psi}}_{1h} = \tau\overline{\boldsymbol{K}}_h^k, \tilde{\boldsymbol{\psi}}_{2h} = \tau\overline{\boldsymbol{M}}_h^k, \tilde{\boldsymbol{\phi}}_h = \tau\overline{\boldsymbol{J}}_h^k$ in (3.4)–(3.8), respectively, then adding the resultants together, we have

$$\begin{aligned}
&\frac{\epsilon_0}{2}\big(\big\|\boldsymbol{E}_h^k\big\|_0^2 - \big\|\boldsymbol{E}_h^{k-1}\big\|_0^2\big) + \frac{\mu_0}{2}\big(\big\|\boldsymbol{H}_h^k\big\|_0^2 - \big\|\boldsymbol{H}_h^{k-1}\big\|_0^2\big) + \frac{1}{2\epsilon_0\omega_p^2}\big(\big\|\boldsymbol{J}_h^k\big\|_0^2 - \big\|\boldsymbol{J}_h^{k-1}\big\|_0^2\big) \\
&\quad + \frac{\tau\nu}{\epsilon_0\omega_p^2}\big\|\overline{\boldsymbol{J}}_h^k\big\|_0^2 + \frac{1}{2\mu_0\omega_0^2 F}\big(\big\|\boldsymbol{K}_h^k\big\|_0^2 - \big\|\boldsymbol{K}_h^{k-1}\big\|_0^2\big) + \frac{\tau\gamma}{\mu_0\omega_0^2 F}\big\|\overline{\boldsymbol{K}}_h^k\big\|_0^2 \\
&\quad + \frac{1}{2\mu_0 F}\big(\big\|\boldsymbol{M}_h^k\big\|_0^2 - \big\|\boldsymbol{M}_h^{k-1}\big\|_0^2\big) = 0,
\end{aligned}$$

which easily leads to (3.9). □

For the Crank-Nicolson scheme (3.4)–(3.8), we can prove the following optimal error estimate.

Theorem 3.2 *Let $(\boldsymbol{E}^m, \boldsymbol{H}^m, \boldsymbol{K}^m, \boldsymbol{M}^m, \boldsymbol{J}^m)$ and $(\boldsymbol{E}_h^m, \boldsymbol{H}_h^m, \boldsymbol{K}_h^m, \boldsymbol{M}_h^m, \boldsymbol{J}_h^m)$ be the analytic and numerical solutions of (2.7)–(2.11) and (3.4)–(3.8) at time t_m, respectively. Under the following regularity assumptions*:

$$\boldsymbol{E}_t, \boldsymbol{J}_t \in L^2\big(0, T; \boldsymbol{H}^l(\mathrm{curl}; \Omega)\big),$$
$$\boldsymbol{E}_{tt}, \boldsymbol{J}_{tt}, \boldsymbol{H}_{tt}, \boldsymbol{K}_{tt}, \boldsymbol{M}_{tt}, \nabla\times\boldsymbol{E}_{tt}, \nabla\times\boldsymbol{H}_{tt} \in L^2\big(0, T; \boldsymbol{L}^2(\Omega)\big),$$
$$\boldsymbol{E}, \boldsymbol{J}, \nabla\times\boldsymbol{E} \in L^\infty\big(0, T; \boldsymbol{H}^l(\mathrm{curl}; \Omega)\big),$$
$$\boldsymbol{H}, \boldsymbol{K}, \boldsymbol{M} \in L^\infty\big(0, T; \boldsymbol{H}^l(\Omega)\big),$$

there exists a constant $C>0$ independent of the mesh size h and time step τ, such that

$$\max_{n\geq 1}\biggl(\epsilon_0\|\boldsymbol{E}^n-\boldsymbol{E}_h^n\|_0^2+\mu_0\|\boldsymbol{H}^n-\boldsymbol{H}_h^n\|_0^2+\frac{1}{\epsilon_0\omega_p^2}\|\boldsymbol{J}^n-\boldsymbol{J}_h^n\|_0^2$$
$$+\frac{1}{\mu_0\omega_0^2F}\|\boldsymbol{K}^n-\boldsymbol{K}_h^n\|_0^2+\frac{1}{\mu_0F}\|\boldsymbol{M}^n-\boldsymbol{M}_h^n\|_0^2\biggr)\leq C\bigl(h^{2l}+\tau^4\bigr),$$

where $l\geq 1$ is the order of the basis functions in spaces $\boldsymbol{U}_h$ and $\boldsymbol{V}_h$.

Proof Integrating (2.7)–(2.11) from t_{k-1} to t_k, then multiplying test functions $\boldsymbol{\phi}_h\in\boldsymbol{V}_h^0,\boldsymbol{\psi}_h,\tilde{\boldsymbol{\psi}}_{1h},\tilde{\boldsymbol{\psi}}_{2h}\in\boldsymbol{U}_h,\tilde{\boldsymbol{\phi}}_h\in\boldsymbol{V}_h$ and integrating the resultant equations over domain Ω, we obtain

$$\epsilon_0\bigl(\delta_\tau\boldsymbol{E}^k,\boldsymbol{\phi}_h\bigr)-\left(\frac{1}{\tau}\int_{I_k}\boldsymbol{H},\nabla\times\boldsymbol{\phi}_h\right)+\left(\frac{1}{\tau}\int_{I_k}\boldsymbol{J},\boldsymbol{\phi}_h\right)=0, \tag{3.10}$$

$$\mu_0\bigl(\delta_\tau\boldsymbol{H}^k,\boldsymbol{\psi}_h\bigr)+\left(\frac{1}{\tau}\int_{I_k}\nabla\times\boldsymbol{E},\boldsymbol{\psi}_h\right)+\left(\frac{1}{\tau}\int_{I_k}\boldsymbol{K},\boldsymbol{\psi}_h\right)=0, \tag{3.11}$$

$$\frac{1}{\mu_0\omega_0^2F}\bigl(\delta_\tau\boldsymbol{K}^k,\tilde{\boldsymbol{\psi}}_{1h}\bigr)+\frac{\gamma}{\mu_0\omega_0^2F}\left(\frac{1}{\tau}\int_{I_k}\boldsymbol{K},\tilde{\boldsymbol{\psi}}_{1h}\right)+\frac{1}{\mu_0F}\left(\frac{1}{\tau}\int_{I_k}\boldsymbol{M},\tilde{\boldsymbol{\psi}}_{1h}\right)$$
$$=\left(\frac{1}{\tau}\int_{I_k}\boldsymbol{H},\tilde{\boldsymbol{\psi}}_{1h}\right), \tag{3.12}$$

$$\frac{1}{\mu_0F}\bigl(\delta_\tau\boldsymbol{M}^k,\tilde{\boldsymbol{\psi}}_{2h}\bigr)=\frac{1}{\mu_0F}\left(\frac{1}{\tau}\int_{I_k}\boldsymbol{K},\tilde{\boldsymbol{\psi}}_{2h}\right),$$
$$\frac{1}{\epsilon_0\omega_p^2}\bigl(\delta_\tau\boldsymbol{J}^k,\tilde{\boldsymbol{\phi}}_h\bigr)+\frac{\nu}{\epsilon_0\omega_p^2}\left(\frac{1}{\tau}\int_{I_k}\boldsymbol{J},\tilde{\boldsymbol{\phi}}_h\right)=\left(\frac{1}{\tau}\int_{I_k}\boldsymbol{E},\tilde{\boldsymbol{\phi}}_h\right). \tag{3.13}$$

Let us denote

$$\xi_h^k=\Pi_h\boldsymbol{E}^k-\boldsymbol{E}_h^k,\qquad \eta_h^k=P_h\boldsymbol{H}^k-\boldsymbol{H}_h^k,\qquad \tilde{\xi}_{1h}^k=P_h\boldsymbol{K}^k-\boldsymbol{K}_h^k,$$
$$\tilde{\xi}_{2h}^k=P_h\boldsymbol{M}^k-\boldsymbol{M}_h^k,\qquad \zeta_h^k=\Pi_h\boldsymbol{J}^k-\boldsymbol{J}_h^k.$$

Subtracting (3.10)–(3.13) from (3.4)–(3.8) gives us the error equations

$$\epsilon_0\bigl(\delta_\tau\xi_h^k,\boldsymbol{\phi}_h\bigr)-\bigl(\overline{\eta}_h^k,\nabla\times\boldsymbol{\phi}_h\bigr)+\bigl(\overline{\zeta}_h^k,\boldsymbol{\phi}_h\bigr)$$
$$=\epsilon_0\bigl(\delta_\tau\bigl(\Pi_h\boldsymbol{E}^k-\boldsymbol{E}^k\bigr),\boldsymbol{\phi}_h\bigr)-\left(P_h\overline{\boldsymbol{H}}^k-\frac{1}{\tau}\int_{I_k}\boldsymbol{H},\nabla\times\boldsymbol{\phi}_h\right)$$
$$+\left(\Pi_h\overline{\boldsymbol{J}}^k-\frac{1}{\tau}\int_{I_k}\boldsymbol{J},\boldsymbol{\phi}_h\right), \tag{3.14}$$

$$\mu_0\bigl(\delta_\tau\eta_h^k,\boldsymbol{\psi}_h\bigr)+\bigl(\nabla\times\overline{\xi}_h^k,\boldsymbol{\psi}_h\bigr)+\bigl(\overline{\tilde{\xi}}_{1h}^k,\boldsymbol{\psi}_h\bigr)$$
$$=\mu_0\bigl(\delta_\tau\bigl(P_h\boldsymbol{H}^k-\boldsymbol{H}^k\bigr),\boldsymbol{\psi}_h\bigr)+\left(\nabla\times\left(\Pi_h\overline{\boldsymbol{E}}^k-\frac{1}{\tau}\int_{I_k}\boldsymbol{E}\right),\boldsymbol{\psi}_h\right)$$
$$+\left(P_h\overline{\boldsymbol{K}}^k-\frac{1}{\tau}\int_{I_k}\boldsymbol{K},\boldsymbol{\psi}_h\right), \tag{3.15}$$

$$\frac{1}{\mu_0\omega_0^2 F}\big(\delta_\tau\tilde{\xi}_{1h}^k,\tilde{\boldsymbol{\psi}}_{1h}\big)+\frac{\gamma}{\mu_0\omega_0^2 F}\big(\overline{\tilde{\xi}}_{1h}^k,\tilde{\boldsymbol{\psi}}_{1h}\big)+\frac{1}{\mu_0 F}\big(\overline{\tilde{\xi}}_{2h}^k,\tilde{\boldsymbol{\psi}}_{1h}\big)-\big(\overline{\eta}_h^k,\tilde{\boldsymbol{\psi}}_{1h}\big)$$
$$=\frac{1}{\mu_0\omega_0^2 F}\big(\delta_\tau\big(P_h\boldsymbol{K}^k-\boldsymbol{K}^k\big),\tilde{\boldsymbol{\psi}}_{1h}\big)+\frac{\gamma}{\mu_0\omega_0^2 F}\left(P_h\overline{\boldsymbol{K}}^k-\frac{1}{\tau}\int_{I_k}\boldsymbol{K},\tilde{\boldsymbol{\psi}}_{1h}\right)$$
$$+\frac{1}{\mu_0 F}\left(P_h\overline{\boldsymbol{M}}^k-\frac{1}{\tau}\int_{I_k}\boldsymbol{M},\tilde{\boldsymbol{\psi}}_{1h}\right)-\left(P_h\overline{\boldsymbol{H}}^k-\frac{1}{\tau}\int_{I_k}\boldsymbol{H},\tilde{\boldsymbol{\psi}}_{1h}\right), \tag{3.16}$$

$$\frac{1}{\mu_0 F}\big(\delta_\tau\tilde{\xi}_{2h}^k,\tilde{\boldsymbol{\psi}}_{2h}\big)-\frac{1}{\mu_0 F}\big(\overline{\tilde{\xi}}_{1h}^k,\tilde{\boldsymbol{\psi}}_{2h}\big)$$
$$=\frac{1}{\mu_0 F}\big(\delta_\tau\big(P_h\boldsymbol{M}^k-\boldsymbol{M}^k\big),\tilde{\boldsymbol{\psi}}_{2h}\big)-\frac{1}{\mu_0 F}\left(P_h\overline{\boldsymbol{K}}^k-\frac{1}{\tau}\int_{I_k}\boldsymbol{K},\tilde{\boldsymbol{\psi}}_{2h}\right), \tag{3.17}$$

$$\frac{1}{\epsilon_0\omega_p^2}\big(\delta_\tau\zeta_h^k,\tilde{\boldsymbol{\phi}}_h\big)+\frac{\nu}{\epsilon_0\omega_p^2}\big(\overline{\zeta}_h^k,\tilde{\boldsymbol{\phi}}_h\big)-\big(\overline{\xi}_h^k,\tilde{\boldsymbol{\phi}}_h\big)$$
$$=\frac{1}{\epsilon_0\omega_p^2}\big(\delta_\tau\big(\Pi_h\boldsymbol{J}^k-\boldsymbol{J}^k\big),\tilde{\boldsymbol{\phi}}_h\big)+\frac{\nu}{\epsilon_0\omega_p^2}\left(\Pi_h\overline{\boldsymbol{J}}^k-\frac{1}{\tau}\int_{I_k}\boldsymbol{J},\tilde{\boldsymbol{\phi}}_h\right)$$
$$-\left(\Pi_h\overline{\boldsymbol{E}}^k-\frac{1}{\tau}\int_{I_k}\boldsymbol{E},\tilde{\boldsymbol{\phi}}_h\right). \tag{3.18}$$

Choosing $\boldsymbol{\phi}_h=\tau\overline{\xi}_h^k$, $\boldsymbol{\psi}_h=\tau\overline{\eta}_h^k$, $\tilde{\boldsymbol{\psi}}_{1h}=\tau\overline{\tilde{\xi}}_{1h}^k$, $\tilde{\boldsymbol{\psi}}_{2h}=\tau\overline{\tilde{\xi}}_{2h}^k$, $\tilde{\boldsymbol{\phi}}_h=\tau\overline{\zeta}_h^k$ in (3.14)–(3.18), respectively, then adding the resultants together and using the projection property, we have

$$\frac{\epsilon_0}{2}\big(\|\xi_h^k\|_0^2-\|\xi_h^{k-1}\|_0^2\big)+\frac{\mu_0}{2}\big(\|\eta_h^k\|_0^2-\|\eta_h^{k-1}\|_0^2\big)+\frac{1}{2\epsilon_0\omega_p^2}\big(\|\zeta_h^k\|_0^2-\|\zeta_h^{k-1}\|_0^2\big)+\frac{\tau\nu}{\epsilon_0\omega_p^2}\|\overline{\zeta}_h^k\|_0^2$$
$$+\frac{1}{2\mu_0\omega_0^2 F}\big(\|\tilde{\xi}_{1h}^k\|_0^2-\|\tilde{\xi}_{1h}^{k-1}\|_0^2\big)+\frac{\tau\gamma}{\mu_0\omega_0^2 F}\|\overline{\tilde{\xi}}_{1h}^k\|_0^2+\frac{1}{2\mu_0 F}\big(\|\tilde{\xi}_{2h}^k\|_0^2-\|\tilde{\xi}_{2h}^{k-1}\|_0^2\big)$$
$$=\tau\epsilon_0\big(\delta_\tau\big(\Pi_h\boldsymbol{E}^k-\boldsymbol{E}^k\big),\overline{\xi}_h^k\big)-\tau\left(\overline{\boldsymbol{H}}^k-\frac{1}{\tau}\int_{I_k}\boldsymbol{H},\nabla\times\overline{\xi}_h^k\right)+\tau\left(\Pi_h\overline{\boldsymbol{J}}^k-\frac{1}{\tau}\int_{I_k}\boldsymbol{J},\overline{\xi}_h^k\right)$$
$$+\tau\left(\nabla\times\left(\Pi_h\overline{\boldsymbol{E}}^k-\frac{1}{\tau}\int_{I_k}\boldsymbol{E}\right),\overline{\eta}_h^k\right)+\tau\left(\overline{\boldsymbol{K}}^k-\frac{1}{\tau}\int_{I_k}\boldsymbol{K},\overline{\eta}_h^k\right)$$
$$+\tau\frac{\gamma}{\mu_0\omega_0^2 F}\left(\overline{\boldsymbol{K}}^k-\frac{1}{\tau}\int_{I_k}\boldsymbol{K},\overline{\tilde{\xi}}_{1h}^k\right)+\tau\frac{1}{\mu_0 F}\left(\overline{\boldsymbol{M}}^k-\frac{1}{\tau}\int_{I_k}\boldsymbol{M},\overline{\tilde{\xi}}_{1h}^k\right)$$
$$-\tau\left(\overline{\boldsymbol{H}}^k-\frac{1}{\tau}\int_{I_k}\boldsymbol{H},\overline{\tilde{\xi}}_{1h}^k\right)-\tau\frac{1}{\mu_0 F}\left(\overline{\boldsymbol{K}}^k-\frac{1}{\tau}\int_{I_k}\boldsymbol{K},\overline{\tilde{\xi}}_{2h}^k\right)$$
$$+\tau\frac{1}{\epsilon_0\omega_p^2}\big(\delta_\tau\big(\Pi_h\boldsymbol{J}^k-\boldsymbol{J}^k\big),\overline{\zeta}_h^k\big)+\tau\frac{\nu}{\epsilon_0\omega_p^2}\left(\Pi_h\overline{\boldsymbol{J}}^k-\frac{1}{\tau}\int_{I_k}\boldsymbol{J},\overline{\zeta}_h^k\right)$$
$$-\tau\left(\Pi_h\overline{\boldsymbol{E}}^k-\frac{1}{\tau}\int_{I_k}\boldsymbol{E},\overline{\zeta}_h^k\right). \tag{3.19}$$

The rest proof is standard (see our early work [24]) by estimating each term on the right hand side of (3.19), and using the triangle inequality and the estimates (3.2)–(3.3). □

3.2 The Leap-Frog Scheme

We construct a leap-frog type scheme for solving (2.7)–(2.11): For $k = 1, 2, \ldots$, find $\boldsymbol{E}_h^k \in \boldsymbol{V}_h^0$, $\boldsymbol{J}_h^{k+\frac{1}{2}} \in \boldsymbol{V}_h$, $\boldsymbol{H}_h^{k+\frac{1}{2}}, \boldsymbol{K}_h^k, \boldsymbol{M}_h^{k+\frac{1}{2}} \in \boldsymbol{U}_h$ such that

$$\epsilon_0\left(\frac{\boldsymbol{E}_h^k - \boldsymbol{E}_h^{k-1}}{\tau}, \boldsymbol{\phi}_h\right) - \left(\boldsymbol{H}_h^{k-\frac{1}{2}}, \nabla \times \boldsymbol{\phi}_h\right) + \left(\boldsymbol{J}_h^{k-\frac{1}{2}}, \boldsymbol{\phi}_h\right) = 0, \tag{3.20}$$

$$\mu_0\left(\frac{\boldsymbol{H}_h^{k+\frac{1}{2}} - \boldsymbol{H}_h^{k-\frac{1}{2}}}{\tau}, \boldsymbol{\psi}_h\right) + \left(\nabla \times \boldsymbol{E}_h^k, \boldsymbol{\psi}_h\right) + \left(\boldsymbol{K}_h^k, \boldsymbol{\psi}_h\right) = 0, \tag{3.21}$$

$$\begin{aligned} &\frac{1}{\mu_0\omega_0^2 F}\left(\frac{\boldsymbol{K}_h^k - \boldsymbol{K}_h^{k-1}}{\tau}, \tilde{\boldsymbol{\psi}}_{1h}\right) + \frac{\gamma}{\mu_0\omega_0^2 F}\left(\frac{\boldsymbol{K}_h^k + \boldsymbol{K}_h^{k-1}}{2}, \tilde{\boldsymbol{\psi}}_{1h}\right) + \frac{1}{\mu_0 F}\left(\boldsymbol{M}_h^{k-\frac{1}{2}}, \tilde{\boldsymbol{\psi}}_{1h}\right) \\ &\quad = \left(\boldsymbol{H}_h^{k-\frac{1}{2}}, \tilde{\boldsymbol{\psi}}_{1h}\right), \end{aligned} \tag{3.22}$$

$$\frac{1}{\mu_0 F}\left(\frac{\boldsymbol{M}_h^{k+\frac{1}{2}} - \boldsymbol{M}_h^{k-\frac{1}{2}}}{\tau}, \tilde{\boldsymbol{\psi}}_{2h}\right) = \frac{1}{\mu_0 F}\left(\boldsymbol{K}_h^k, \tilde{\boldsymbol{\psi}}_{2h}\right),$$

$$\frac{1}{\epsilon_0\omega_p^2}\left(\frac{\boldsymbol{J}_h^{k+\frac{1}{2}} - \boldsymbol{J}_h^{k-\frac{1}{2}}}{\tau}, \tilde{\boldsymbol{\phi}}_h\right) + \frac{\nu}{\epsilon_0\omega_p^2}\left(\frac{\boldsymbol{J}_h^{k+\frac{1}{2}} + \boldsymbol{J}_h^{k-\frac{1}{2}}}{2}, \tilde{\boldsymbol{\phi}}_h\right) = \left(\boldsymbol{E}_h^k, \tilde{\boldsymbol{\phi}}_h\right), \tag{3.23}$$

hold true for any $\boldsymbol{\phi}_h \in \boldsymbol{V}_h^0, \boldsymbol{\psi}_h, \tilde{\boldsymbol{\psi}}_{1h}, \tilde{\boldsymbol{\psi}}_{2h} \in \boldsymbol{U}_h, \tilde{\boldsymbol{\phi}}_h \in \boldsymbol{V}_h$, and are subject to the initial approximations

$$\begin{aligned} &\boldsymbol{E}_h^0(\boldsymbol{x}) = \Pi_h \boldsymbol{E}_0(\boldsymbol{x}), \\ &\boldsymbol{H}_h^{\frac{1}{2}}(\boldsymbol{x}) = P_h\left[\boldsymbol{H}_0(\boldsymbol{x}) - \frac{\tau}{2}\mu_0^{-1}\left(\nabla \times \boldsymbol{E}_0(\boldsymbol{x}) + \boldsymbol{K}_0(\boldsymbol{x})\right)\right], \end{aligned} \tag{3.24}$$

$$\begin{aligned} &\boldsymbol{K}_h^0(\boldsymbol{x}) = P_h \boldsymbol{K}_0(\boldsymbol{x}), \qquad \boldsymbol{M}_h^{\frac{1}{2}}(\boldsymbol{x}) = P_h\left[\boldsymbol{M}_0(\boldsymbol{x}) + \frac{\tau}{2}\boldsymbol{K}_0(\boldsymbol{x})\right], \\ &\boldsymbol{J}_h^{\frac{1}{2}}(\boldsymbol{x}) = \Pi_h\left[\boldsymbol{J}_0(\boldsymbol{x}) + \frac{\tau}{2}\left(\epsilon_0\omega_p^2 \boldsymbol{E}_0(\boldsymbol{x}) - \nu \boldsymbol{J}_0(\boldsymbol{x})\right)\right]. \end{aligned} \tag{3.25}$$

First, let us prove the following discrete stability for the leap-frog scheme (3.20)–(3.23).

Lemma 3.3 *Denote $c_v = \frac{1}{\sqrt{\mu_0\epsilon_0}}$ for the speed of light in vacuum, and a constant $c_{inv} > 0$ in the standard inverse estimate*

$$\|\nabla \times \boldsymbol{u}_h\|_0 \le c_{inv} h^{-1} \|\boldsymbol{u}_h\|_0, \quad \forall \boldsymbol{u}_h \in \boldsymbol{V}_h. \tag{3.26}$$

Under the time step constraint

$$\tau = \min\left\{\frac{1}{2\omega_0\sqrt{F}}, \frac{1}{2\omega_0}, \frac{1}{2\omega_p}, \frac{h}{2c_v c_{inv}}\right\}, \tag{3.27}$$

for any $k \geq 1$ we have

$$\epsilon_0\|\boldsymbol{E}_h^k\|_0^2+\mu_0\|\boldsymbol{H}_h^{k+\frac{1}{2}}\|_0^2+\frac{1}{\epsilon_0\omega_p^2}\|\boldsymbol{J}_h^{k+\frac{1}{2}}\|_0^2+\frac{1}{\mu_0\omega_0^2F}\|\boldsymbol{K}_h^k\|_0^2+\frac{1}{\mu_0F}\|\boldsymbol{M}_h^{k+\frac{1}{2}}\|_0^2$$
$$\leq C\left[\epsilon_0\|\boldsymbol{E}_h^0\|_0^2+\mu_0\|\boldsymbol{H}_h^{\frac{1}{2}}\|_0^2+\frac{1}{\epsilon_0\omega_p^2}\|\boldsymbol{J}_h^{\frac{1}{2}}\|_0^2+\frac{1}{\mu_0\omega_0^2F}\|\boldsymbol{K}_h^0\|_0^2+\frac{1}{\mu_0F}\|\boldsymbol{M}_h^{\frac{1}{2}}\|_0^2\right], \quad (3.28)$$

where $C>1$ is independent of h and τ.

Proof Choosing $\boldsymbol{\phi}_h=\tau(\boldsymbol{E}_h^k+\boldsymbol{E}_h^{k-1})$, $\boldsymbol{\psi}_h=\tau(\boldsymbol{H}_h^{k+\frac{1}{2}}+\boldsymbol{H}_h^{k-\frac{1}{2}})$, $\tilde{\boldsymbol{\psi}}_{1h}=\tau(\boldsymbol{K}_h^k+\boldsymbol{K}_h^{k-1})$, $\tilde{\boldsymbol{\psi}}_{2h}=\tau(\boldsymbol{M}_h^{k+\frac{1}{2}}+\boldsymbol{M}_h^{k-\frac{1}{2}})$, $\tilde{\boldsymbol{\phi}}_h=\tau(\boldsymbol{J}_h^{k+\frac{1}{2}}+\boldsymbol{J}_h^{k-\frac{1}{2}})$ in (3.20)–(3.23), respectively, then adding the resultants together, we have

$$\begin{aligned}
&\epsilon_0\big(\|\boldsymbol{E}_h^k\|_0^2-\|\boldsymbol{E}_h^{k-1}\|_0^2\big)+\mu_0\big(\|\boldsymbol{H}_h^{k+\frac{1}{2}}\|_0^2-\|\boldsymbol{H}_h^{k-\frac{1}{2}}\|_0^2\big)+\frac{1}{\epsilon_0\omega_p^2}\big(\|\boldsymbol{J}_h^{k+\frac{1}{2}}\|_0^2-\|\boldsymbol{J}_h^{k-\frac{1}{2}}\|_0^2\big)\\
&\quad+\frac{1}{\mu_0\omega_0^2F}\big(\|\boldsymbol{K}_h^k\|_0^2-\|\boldsymbol{K}_h^{k-1}\|_0^2\big)+\frac{1}{\mu_0F}\big(\|\boldsymbol{M}_h^{k+\frac{1}{2}}\|_0^2-\|\boldsymbol{M}_h^{k-\frac{1}{2}}\|_0^2\big)\\
&\leq\tau\big(\boldsymbol{H}_h^{k-\frac{1}{2}},\nabla\times\big(\boldsymbol{E}_h^k+\boldsymbol{E}_h^{k-1}\big)\big)-\tau\big(\nabla\times\boldsymbol{E}_h^k,\boldsymbol{H}_h^{k+\frac{1}{2}}+\boldsymbol{H}_h^{k-\frac{1}{2}}\big)\\
&\quad-\tau\big(\boldsymbol{J}_h^{k-\frac{1}{2}},\boldsymbol{E}_h^k+\boldsymbol{E}_h^{k-1}\big)+\tau\big(\boldsymbol{E}_h^k,\boldsymbol{J}_h^{k+\frac{1}{2}}+\boldsymbol{J}_h^{k-\frac{1}{2}}\big)-\tau\big(\boldsymbol{K}_h^k,\boldsymbol{H}_h^{k+\frac{1}{2}}+\boldsymbol{H}_h^{k-\frac{1}{2}}\big)\\
&\quad+\tau\big(\boldsymbol{H}_h^{k-\frac{1}{2}},\boldsymbol{K}_h^k+\boldsymbol{K}_h^{k-1}\big)-\frac{\tau}{\mu_0F}\big(\boldsymbol{M}_h^{k-\frac{1}{2}},\boldsymbol{K}_h^k+\boldsymbol{K}_h^{k-1}\big)+\frac{\tau}{\mu_0F}\big(\boldsymbol{K}_h^k,\boldsymbol{M}_h^{k+\frac{1}{2}}+\boldsymbol{M}_h^{k-\frac{1}{2}}\big)\\
&=\tau\big[\big(\boldsymbol{H}_h^{k-\frac{1}{2}},\nabla\times\boldsymbol{E}_h^{k-1}\big)-\big(\boldsymbol{H}_h^{k+\frac{1}{2}},\nabla\times\boldsymbol{E}_h^k\big)\big]+\tau\big[\big(\boldsymbol{E}_h^k,\boldsymbol{J}_h^{k+\frac{1}{2}}\big)-\big(\boldsymbol{E}_h^{k-1},\boldsymbol{J}_h^{k-\frac{1}{2}}\big)\big]\\
&\quad+\tau\big[\big(\boldsymbol{H}_h^{k-\frac{1}{2}},\boldsymbol{K}_h^{k-1}\big)-\big(\boldsymbol{H}_h^{k+\frac{1}{2}},\boldsymbol{K}_h^k\big)\big]+\frac{\tau}{\mu_0F}\big[\big(\boldsymbol{K}_h^k,\boldsymbol{M}_h^{k+\frac{1}{2}}\big)-\big(\boldsymbol{K}_h^{k-1},\boldsymbol{M}_h^{k-\frac{1}{2}}\big)\big].
\end{aligned}\quad (3.29)$$

Summing up (3.29) for k from 1 to n, we obtain

$$\begin{aligned}
&\epsilon_0\big(\|\boldsymbol{E}_h^n\|_0^2-\|\boldsymbol{E}_h^0\|_0^2\big)+\mu_0\big(\|\boldsymbol{H}_h^{n+\frac{1}{2}}\|_0^2-\|\boldsymbol{H}_h^{\frac{1}{2}}\|_0^2\big)+\frac{1}{\epsilon_0\omega_p^2}\big(\|\boldsymbol{J}_h^{n+\frac{1}{2}}\|_0^2-\|\boldsymbol{J}_h^{\frac{1}{2}}\|_0^2\big)\\
&\quad+\frac{1}{\mu_0\omega_0^2F}\big(\|\boldsymbol{K}_h^n\|_0^2-\|\boldsymbol{K}_h^0\|_0^2\big)+\frac{1}{\mu_0F}\big(\|\boldsymbol{M}_h^{n+\frac{1}{2}}\|_0^2-\|\boldsymbol{M}_h^{\frac{1}{2}}\|_0^2\big)\\
&\leq\tau\big[\big(\boldsymbol{H}_h^{\frac{1}{2}},\nabla\times\boldsymbol{E}_h^0\big)-\big(\boldsymbol{H}_h^{n+\frac{1}{2}},\nabla\times\boldsymbol{E}_h^n\big)\big]+\tau\big[\big(\boldsymbol{E}_h^n,\boldsymbol{J}_h^{n+\frac{1}{2}}\big)-\big(\boldsymbol{E}_h^0,\boldsymbol{J}_h^{\frac{1}{2}}\big)\big]\\
&\quad+\tau\big[\big(\boldsymbol{H}_h^{\frac{1}{2}},\boldsymbol{K}_h^0\big)-\big(\boldsymbol{H}_h^{n+\frac{1}{2}},\boldsymbol{K}_h^n\big)\big]+\frac{\tau}{\mu_0F}\big[\big(\boldsymbol{K}_h^n,\boldsymbol{M}_h^{n+\frac{1}{2}}\big)-\big(\boldsymbol{K}_h^0,\boldsymbol{M}_h^{\frac{1}{2}}\big)\big].
\end{aligned}\quad (3.30)$$

Using the inverse estimate (3.26) and the basic arithmetic-geometric mean inequality

$$|ab|\leq\delta a^2+\frac{1}{4\delta}b^2,$$

we have

$$\tau\big(\boldsymbol{H}_h^{n+\frac{1}{2}}, \nabla\times\boldsymbol{E}_h^n\big) = \big(\sqrt{\mu_0}\boldsymbol{H}_h^{n+\frac{1}{2}}, \tau c_v\sqrt{\epsilon_0}\nabla\times\boldsymbol{E}_h^n\big)$$
$$\le \delta_1\mu_0\big\|\boldsymbol{H}_h^{n+\frac{1}{2}}\big\|_0^2 + \frac{(\tau c_v c_{inv}h^{-1})^2}{4\delta_1}\epsilon_0\big\|\boldsymbol{E}_h^n\big\|_0^2.$$

Similarly, we have

$$\tau\big(\boldsymbol{E}_h^n, \boldsymbol{J}_h^{n+\frac{1}{2}}\big) = \left(\tau\omega_p\sqrt{\epsilon_0}\boldsymbol{E}_h^n, \frac{1}{\sqrt{\epsilon_0\omega_p^2}}\boldsymbol{J}_h^{n+\frac{1}{2}}\right)$$
$$\le \frac{\delta_2}{\epsilon_0\omega_p^2}\big\|\boldsymbol{J}_h^{n+\frac{1}{2}}\big\|_0^2 + \frac{(\tau\omega_p)^2}{4\delta_2}\epsilon_0\big\|\boldsymbol{E}_h^n\big\|_0^2,$$

$$\tau\big(\boldsymbol{H}_h^{n+\frac{1}{2}}, \boldsymbol{K}_h^n\big) = \left(\sqrt{\mu_0}\boldsymbol{H}_h^{n+\frac{1}{2}}, \frac{\tau\omega_0\sqrt{F}}{\sqrt{\mu_0\omega_0^2F}}\boldsymbol{K}_h^n\right)$$
$$\le \delta_3\mu_0\big\|\boldsymbol{H}_h^{n+\frac{1}{2}}\big\|_0^2 + \frac{(\tau\omega_0\sqrt{F})^2}{4\delta_3}\cdot\frac{1}{\mu_0\omega_0 F}\big\|\boldsymbol{K}_h^n\big\|_0^2,$$

and

$$\frac{\tau}{\mu_0F}\big(\boldsymbol{K}_h^n, \boldsymbol{M}_h^{n+\frac{1}{2}}\big) = \left(\frac{1}{\mu_0\omega_0^2F}\boldsymbol{K}_h^n, \frac{\tau\omega_0}{\sqrt{\mu_0F}}\boldsymbol{M}_h^{n+\frac{1}{2}}\right)$$
$$\le \delta_4\cdot\frac{1}{\mu_0\omega_0^2F}\big\|\boldsymbol{K}_h^n\big\|_0^2 + \frac{(\tau\omega_0)^2}{4\delta_4}\cdot\frac{1}{\mu_0F}\big\|\boldsymbol{M}_h^{n+\frac{1}{2}}\big\|_0^2.$$

Substituting the above inequalities into (3.30), we have

$$\begin{aligned}
&\left(1-\frac{(\tau c_v c_{inv}h^{-1})^2}{4\delta_1}-\frac{(\tau\omega_p)^2}{4\delta_2}\right)\epsilon_0\big\|\boldsymbol{E}_h^n\big\|_0^2 + (1-\delta_2-\delta_3)\mu_0\big\|\boldsymbol{H}_h^{n+\frac{1}{2}}\big\|_0^2\\
&\quad + (1-\delta_2)\frac{1}{\epsilon_0\omega_p^2}\big\|\boldsymbol{J}_h^{n+\frac{1}{2}}\big\|_0^2\\
&\quad + \left(1-\frac{(\tau\omega_0\sqrt{F})^2}{4\delta_3}-\delta_4\right)\frac{1}{\mu_0\omega_0^2F}\big\|\boldsymbol{K}_h^n\big\|_0^2 + \left(1-\frac{(\tau\omega_0)^2}{4\delta_4}\right)\frac{1}{\mu_0F}\big\|\boldsymbol{M}_h^{n+\frac{1}{2}}\big\|_0^2\\
&\le \epsilon_0\big\|\boldsymbol{E}_h^0\big\|_0^2 + \mu_0\big\|\boldsymbol{H}_h^{\frac{1}{2}}\big\|_0^2 + \frac{1}{\epsilon_0\omega_p^2}\big\|\boldsymbol{J}_h^{\frac{1}{2}}\big\|_0^2 + \frac{1}{\mu_0\omega_0^2F}\big\|\boldsymbol{K}_h^0\big\|_0^2 + \frac{1}{\mu_0F}\big\|\boldsymbol{M}_h^{\frac{1}{2}}\big\|_0^2\\
&\quad + \tau\big(\boldsymbol{H}_h^{\frac{1}{2}}, \nabla\times\boldsymbol{E}_h^0\big) - \tau\big(\boldsymbol{E}_h^0, \boldsymbol{J}_h^{\frac{1}{2}}\big) + \tau\big(\boldsymbol{H}_h^{\frac{1}{2}}, \boldsymbol{K}_h^0\big) - \tau\big(\boldsymbol{K}_h^0, \boldsymbol{M}_h^{\frac{1}{2}}\big).
\end{aligned}\tag{3.31}$$

Under the choice $\delta_1=\delta_2=\delta_3=\delta_4=\frac{1}{4}$, and

$$\tau = \min\left\{\frac{1}{2\omega_0\sqrt{F}}, \frac{1}{2\omega_0}, \frac{1}{2\omega_p}, \frac{h}{2c_vc_{inv}}\right\},$$

we can easily see that the coefficients on the left hand side of (3.31) are all larger than $\frac{1}{2}$, which easily leads to the stability (3.28). □

For the leap-frog scheme (3.20)–(3.23), we can prove the following optimal error estimate.

Theorem 3.4 *Let* $(\boldsymbol{E}^m, \boldsymbol{H}^{m+\frac{1}{2}}, \boldsymbol{K}^m, \boldsymbol{M}^{m+\frac{1}{2}}, \boldsymbol{J}^{m+\frac{1}{2}})$ *and* $(\boldsymbol{E}_h^m, \boldsymbol{H}_h^{m+\frac{1}{2}}, \boldsymbol{K}_h^m, \boldsymbol{M}_h^{m+\frac{1}{2}}, \boldsymbol{J}_h^{m+\frac{1}{2}})$ *be the analytic and numerical solutions of* (2.7)–(2.11) *and* (3.20)–(3.23), *respectively. Under the same regularity assumptions as Theorem* 3.2, *there exists a constant* $C > 0$ *independent of* h *and* τ *such that*

$$\max_{n\ge 1}\bigg(\epsilon_0\big\|\boldsymbol{E}^n-\boldsymbol{E}_h^n\big\|_0^2+\mu_0\big\|\boldsymbol{H}^{n+\frac{1}{2}}-\boldsymbol{H}_h^{n+\frac{1}{2}}\big\|_0^2+\frac{1}{\epsilon_0\omega_p^2}\big\|\boldsymbol{J}^{n+\frac{1}{2}}-\boldsymbol{J}_h^{n+\frac{1}{2}}\big\|_0^2$$
$$+\frac{1}{\mu_0\omega_0^2F}\big\|\boldsymbol{K}^n-\boldsymbol{K}_h^n\big\|_0^2+\frac{1}{\mu_0F}\big\|\boldsymbol{M}^{n+\frac{1}{2}}-\boldsymbol{M}_h^{n+\frac{1}{2}}\big\|_0^2\bigg)\le C\big(h^{2l}+\tau^4\big),$$

where $l \ge 1$ *is the order of the basis functions in spaces* $\boldsymbol{U}_h$ *and* $\boldsymbol{V}_h$.

Proof Integrating (2.7) and (2.9) from t_{k-1} to t_k, (2.8), (2.10)–(2.11) from $t_{k-\frac{1}{2}}$ to $t_{k+\frac{1}{2}}$, then multiplying proper test functions $\boldsymbol{\phi}_h \in \boldsymbol{V}_h^0$, $\boldsymbol{\psi}_h, \tilde{\boldsymbol{\psi}}_{1h}, \tilde{\boldsymbol{\psi}}_{2h} \in \boldsymbol{U}_h$, $\tilde{\boldsymbol{\phi}}_h \in \boldsymbol{V}_h$ and integrating the resultants over domain Ω, we obtain

$$\epsilon_0\bigg(\frac{\boldsymbol{E}^k-\boldsymbol{E}^{k-1}}{\tau},\boldsymbol{\phi}_h\bigg)-\bigg(\frac{1}{\tau}\int_{t_{k-1}}^{t_k}\boldsymbol{H},\nabla\times\boldsymbol{\phi}_h\bigg)+\bigg(\frac{1}{\tau}\int_{t_{k-1}}^{t_k}\boldsymbol{J},\boldsymbol{\phi}_h\bigg)=0, \tag{3.32}$$

$$\mu_0\bigg(\frac{\boldsymbol{H}^{k+\frac{1}{2}}-\boldsymbol{H}^{k-\frac{1}{2}}}{\tau},\boldsymbol{\psi}_h\bigg)+\bigg(\frac{1}{\tau}\int_{t_{k-\frac{1}{2}}}^{t_{k+\frac{1}{2}}}\nabla\times\boldsymbol{E},\boldsymbol{\psi}_h\bigg)+\bigg(\frac{1}{\tau}\int_{t_{k-\frac{1}{2}}}^{t_{k+\frac{1}{2}}}\boldsymbol{K},\boldsymbol{\psi}_h\bigg)=0, \tag{3.33}$$

$$\frac{1}{\mu_0\omega_0^2F}\bigg(\frac{\boldsymbol{K}^k-\boldsymbol{K}^{k-1}}{\tau},\tilde{\boldsymbol{\psi}}_{1h}\bigg)+\frac{\gamma}{\mu_0\omega_0^2F}\bigg(\frac{1}{\tau}\int_{t_{k-1}}^{t_k}\boldsymbol{K},\tilde{\boldsymbol{\psi}}_{1h}\bigg)+\frac{1}{\mu_0F}\bigg(\frac{1}{\tau}\int_{t_{k-1}}^{t_k}\boldsymbol{M},\tilde{\boldsymbol{\psi}}_{1h}\bigg)$$
$$=\bigg(\frac{1}{\tau}\int_{t_{k-1}}^{t_k}\boldsymbol{H},\tilde{\boldsymbol{\psi}}_{1h}\bigg), \tag{3.34}$$

$$\frac{1}{\mu_0F}\bigg(\frac{\boldsymbol{M}^{k+\frac{1}{2}}-\boldsymbol{M}^{k-\frac{1}{2}}}{\tau},\tilde{\boldsymbol{\psi}}_{2h}\bigg)=\frac{1}{\mu_0F}\bigg(\frac{1}{\tau}\int_{t_{k-\frac{1}{2}}}^{t_{k+\frac{1}{2}}}\boldsymbol{K},\tilde{\boldsymbol{\psi}}_{2h}\bigg),$$

$$\frac{1}{\epsilon_0\omega_p^2}\bigg(\frac{\boldsymbol{J}^{k+\frac{1}{2}}-\boldsymbol{J}^{k-\frac{1}{2}}}{\tau},\tilde{\boldsymbol{\phi}}_h\bigg)+\frac{\nu}{\epsilon_0\omega_p^2}\bigg(\frac{1}{\tau}\int_{t_{k-\frac{1}{2}}}^{t_{k+\frac{1}{2}}}\boldsymbol{J},\tilde{\boldsymbol{\phi}}_h\bigg)=\bigg(\frac{1}{\tau}\int_{t_{k-\frac{1}{2}}}^{t_{k+\frac{1}{2}}}\boldsymbol{E},\tilde{\boldsymbol{\phi}}_h\bigg). \tag{3.35}$$

Let us denote

$$\xi_h^k=\Pi_h\boldsymbol{E}^k-\boldsymbol{E}_h^k,\qquad \eta_h^k=P_h\boldsymbol{H}^k-\boldsymbol{H}_h^k,\qquad \tilde{\xi}_{1h}^k=P_h\boldsymbol{K}^k-\boldsymbol{K}_h^k,$$
$$\tilde{\xi}_{2h}^k=P_h\boldsymbol{M}^k-\boldsymbol{M}_h^k,\qquad \zeta_h^k=\Pi_h\boldsymbol{J}^k-\boldsymbol{J}_h^k.$$

Subtracting (3.32)–(3.35) from (3.20)–(3.23) gives us the error equations:

$$\epsilon_0\big(\delta_\tau\xi_h^k,\boldsymbol{\phi}_h\big)-\big(\eta_h^{k-\frac{1}{2}},\nabla\times\boldsymbol{\phi}_h\big)+\big(\zeta_h^{k-\frac{1}{2}},\boldsymbol{\phi}_h\big)=\epsilon_0\big(\delta_\tau\big(\Pi_h\boldsymbol{E}^k-\boldsymbol{E}^k\big),\boldsymbol{\phi}_h\big)$$
$$-\bigg(P_h\boldsymbol{H}^{k-\frac{1}{2}}-\frac{1}{\tau}\int_{t_{k-1}}^{t_k}\boldsymbol{H},\nabla\times\boldsymbol{\phi}_h\bigg)+\bigg(\Pi_h\boldsymbol{J}^{k-\frac{1}{2}}-\frac{1}{\tau}\int_{t_{k-1}}^{t_k}\boldsymbol{J},\boldsymbol{\phi}_h\bigg), \tag{3.36}$$

$$\mu_0\big(\delta_\tau \eta_h^{k+\frac{1}{2}}, \boldsymbol{\psi}_h\big) + \big(\nabla\times\xi_h^k, \boldsymbol{\psi}_h\big) + \big(\tilde{\xi}_{1h}^k, \boldsymbol{\psi}_h\big)$$
$$= \mu_0\big(\delta_\tau\big(P_h\boldsymbol{H}^{k+\frac{1}{2}} - \boldsymbol{H}^{k+\frac{1}{2}}\big), \boldsymbol{\psi}_h\big)$$
$$+ \left(\nabla\times\left(\Pi_h\boldsymbol{E}^k - \frac{1}{\tau}\int_{t_{k-\frac{1}{2}}}^{t_{k+\frac{1}{2}}}\boldsymbol{E}\right), \boldsymbol{\psi}_h\right) + \left(P_h\boldsymbol{K}^k - \frac{1}{\tau}\int_{t_{k-\frac{1}{2}}}^{t_{k+\frac{1}{2}}}\boldsymbol{K}, \boldsymbol{\psi}_h\right), \tag{3.37}$$

$$\frac{1}{\mu_0\omega_0^2F}\big(\delta_\tau\tilde{\xi}_{1h}^k, \tilde{\boldsymbol{\psi}}_{1h}\big) + \frac{\gamma}{\mu_0\omega_0^2F}\big(\overline{\tilde{\xi}}_{1h}^{k-\frac{1}{2}}, \tilde{\boldsymbol{\psi}}_{1h}\big) + \frac{1}{\mu_0F}\big(\tilde{\xi}_{2h}^{k-\frac{1}{2}}, \tilde{\boldsymbol{\psi}}_{1h}\big) - \big(\eta_h^{k-\frac{1}{2}}, \tilde{\boldsymbol{\psi}}_{1h}\big)$$
$$= \frac{1}{\mu_0\omega_0^2F}\big(\delta_\tau\big(P_h\boldsymbol{K}^k - \boldsymbol{K}^k\big), \tilde{\boldsymbol{\psi}}_{1h}\big) + \frac{\gamma}{\mu_0\omega_0^2F}\left(P_h\overline{\boldsymbol{K}}^{k-\frac{1}{2}} - \frac{1}{\tau}\int_{t_{k-1}}^{t_k}\boldsymbol{K}, \tilde{\boldsymbol{\psi}}_{1h}\right)$$
$$+ \frac{1}{\mu_0F}\left(P_h\boldsymbol{M}^{k-\frac{1}{2}} - \frac{1}{\tau}\int_{t_{k-1}}^{t_k}\boldsymbol{M}, \tilde{\boldsymbol{\psi}}_{1h}\right) - \left(P_h\boldsymbol{H}^{k-\frac{1}{2}} - \frac{1}{\tau}\int_{t_{k-1}}^{t_k}\boldsymbol{H}, \tilde{\boldsymbol{\psi}}_{1h}\right), \tag{3.38}$$

$$\frac{1}{\mu_0F}\big(\delta_\tau\tilde{\xi}_{2h}^{k+\frac{1}{2}}, \tilde{\boldsymbol{\psi}}_{2h}\big) - \frac{1}{\mu_0F}\big(\tilde{\xi}_{1h}^k, \tilde{\boldsymbol{\psi}}_{2h}\big)$$
$$= \frac{1}{\mu_0F}\big(\delta_\tau\big(P_h\boldsymbol{M}^{k+\frac{1}{2}} - \boldsymbol{M}^{k+\frac{1}{2}}\big), \tilde{\boldsymbol{\psi}}_{2h}\big) - \frac{1}{\mu_0F}\left(P_h\boldsymbol{K}^k - \frac{1}{\tau}\int_{t_{k-\frac{1}{2}}}^{t_{k+\frac{1}{2}}}\boldsymbol{K}, \tilde{\boldsymbol{\psi}}_{2h}\right), \tag{3.39}$$

$$\frac{1}{\epsilon_0\omega_p^2}\big(\delta_\tau\zeta_h^{k+\frac{1}{2}}, \tilde{\boldsymbol{\phi}}_h\big) + \frac{\nu}{\epsilon_0\omega_p^2}\big(\overline{\zeta}_h^k, \tilde{\boldsymbol{\phi}}_h\big) - \big(\xi_h^k, \tilde{\boldsymbol{\phi}}_h\big) = \frac{1}{\epsilon_0\omega_p^2}\big(\delta_\tau\big(\Pi_h\boldsymbol{J}^{k+\frac{1}{2}} - \boldsymbol{J}^{k+\frac{1}{2}}\big), \tilde{\boldsymbol{\phi}}_h\big)$$
$$+ \frac{\nu}{\epsilon_0\omega_p^2}\left(\Pi_h\overline{\boldsymbol{J}}^k - \frac{1}{\tau}\int_{t_{k-\frac{1}{2}}}^{t_{k+\frac{1}{2}}}\boldsymbol{J}, \tilde{\boldsymbol{\phi}}_h\right) - \left(\Pi_h\boldsymbol{E}^k - \frac{1}{\tau}\int_{t_{k-\frac{1}{2}}}^{t_{k+\frac{1}{2}}}\boldsymbol{E}, \tilde{\boldsymbol{\phi}}_h\right). \tag{3.40}$$

Choosing $\boldsymbol{\phi}_h = \tau\overline{\xi}_h^{k-\frac{1}{2}}, \boldsymbol{\psi}_h = \tau\overline{\eta}_h^k, \tilde{\boldsymbol{\psi}}_{1h} = \tau\overline{\tilde{\xi}}_{1h}^{k-\frac{1}{2}}, \tilde{\boldsymbol{\psi}}_{2h} = \tau\overline{\tilde{\xi}}_{2h}^k, \tilde{\boldsymbol{\phi}}_h = \tau\overline{\zeta}_h^k$ in (3.36)–(3.40), respectively, then adding the resultants together and using the projection property of P_h, we have

$$\frac{\epsilon_0}{2}\big(\|\xi_h^k\|_0^2 - \|\xi_h^{k-1}\|_0^2\big) + \frac{\mu_0}{2}\big(\|\eta_h^{k+\frac{1}{2}}\|_0^2 - \|\eta_h^{k-\frac{1}{2}}\|_0^2\big) + \frac{1}{2\epsilon_0\omega_p^2}\big(\|\zeta_h^k\|_0^2 - \|\zeta_h^{k-1}\|_0^2\big)$$
$$+ \frac{1}{2\mu_0\omega_0^2F}\big(\|\tilde{\xi}_{1h}^k\|_0^2 - \|\tilde{\xi}_{1h}^{k-1}\|_0^2\big) + \frac{1}{2\mu_0F}\big(\|\tilde{\xi}_{2h}^{k+\frac{1}{2}}\|_0^2 - \|\tilde{\xi}_{2h}^{k-\frac{1}{2}}\|_0^2\big)$$
$$\le \tau\epsilon_0\big(\delta_\tau\big(\Pi_h\boldsymbol{E}^k - \boldsymbol{E}^k\big), \overline{\xi}_h^{k-\frac{1}{2}}\big) - \tau\left(\boldsymbol{H}^{k-\frac{1}{2}} - \frac{1}{\tau}\int_{t_{k-1}}^{t_k}\boldsymbol{H}, \nabla\times\overline{\xi}_h^{k-\frac{1}{2}}\right)$$
$$+ \tau\left(\Pi_h\boldsymbol{J}^{k-\frac{1}{2}} - \frac{1}{\tau}\int_{t_{k-1}}^{t_k}\boldsymbol{J}, \overline{\xi}_h^{k-\frac{1}{2}}\right)$$
$$+ \tau\left(\nabla\times\left(\Pi_h\boldsymbol{E}^k - \frac{1}{\tau}\int_{t_{k-\frac{1}{2}}}^{t_{k+\frac{1}{2}}}\boldsymbol{E}\right), \overline{\eta}_h^k\right) + \tau\left(\boldsymbol{K}^k - \frac{1}{\tau}\int_{t_{k-\frac{1}{2}}}^{t_{k+\frac{1}{2}}}\boldsymbol{K}, \overline{\eta}_h^k\right)$$
$$+ \tau\frac{\gamma}{\mu_0\omega_0^2F}\left(\overline{\boldsymbol{K}}^{k-\frac{1}{2}} - \frac{1}{\tau}\int_{t_{k-1}}^{t_k}\boldsymbol{K}, \overline{\tilde{\xi}}_{1h}^{k-\frac{1}{2}}\right) + \tau\frac{1}{\mu_0F}\left(\boldsymbol{M}^{k-\frac{1}{2}} - \frac{1}{\tau}\int_{t_{k-1}}^{t_k}\boldsymbol{M}, \overline{\tilde{\xi}}_{1h}^{k-\frac{1}{2}}\right)$$

$$
\begin{aligned}
&- \tau\left(\boldsymbol{H}^{k-\frac{1}{2}} - \frac{1}{\tau}\int_{t_{k-1}}^{t_k} \boldsymbol{H}, \overline{\xi}_{1h}^{k-\frac{1}{2}}\right) - \frac{\tau}{\mu_0 F}\left(\boldsymbol{K}^k - \frac{1}{\tau}\int_{t_{k-\frac{1}{2}}}^{t_{k+\frac{1}{2}}} \boldsymbol{K}, \overline{\xi}_{2h}^{k}\right)\\
&+ \frac{\tau}{\epsilon_0\omega_p^2}\left(\delta_\tau\left(\Pi_h \boldsymbol{J}^{k+\frac{1}{2}} - \boldsymbol{J}^{k+\frac{1}{2}}\right), \overline{\zeta}_h^k\right)\\
&+ \tau\frac{\nu}{\epsilon_0\omega_p^2}\left(\Pi_h \overline{\boldsymbol{J}}^k - \frac{1}{\tau}\int_{t_{k-\frac{1}{2}}}^{t_{k+\frac{1}{2}}} \boldsymbol{J}, \overline{\zeta}_h^k\right) - \tau\left(\Pi_h \boldsymbol{E}^k - \frac{1}{\tau}\int_{t_{k-\frac{1}{2}}}^{t_{k+\frac{1}{2}}} \boldsymbol{E}, \overline{\zeta}_h^k\right). \qquad (3.41)
\end{aligned}
$$

The rest proof follows similarly to our early work [23] by estimating each term on the right hand side of (3.41), and using the triangle inequality and the estimates (3.2)–(3.3). □

Remark 3.1 We want to remark that the Crank-Nicolson scheme (3.4)–(3.8) has an non-symmetric linear system of as many as 15 unknown functions (five unknown 3D variables), which results a very large-scale system even for linear edge elements. Hence direct solving the coupled system is quite challenging. In this aspect the leap-frog scheme (3.20)–(3.23) is more practical, since each time we only need solve one unknown variable. Of course, we have the CFL time step constraint. More efficient algorithms will be explorered in the future.

4 Numerical Results

In this section, we implemented the leap-frog scheme (3.20)–(3.23) for the lowest-order Raviart-Thomas-Nedelec cubic element (i.e., $l = 1$ in $\boldsymbol{U}_h$ and $\boldsymbol{V}_h$) to confirm our theoretical analysis and effectiveness of our algorithm. For simplicity, we assume that Ω is the unit cube $[0, 1]^3$ and the time interval is $I = [0, 1]$.

To rigorously check the convergence rate, we construct an analytical solution of (2.7)–(2.11) with all physical parameters in (2.7)–(2.11) being one except that $\gamma = \omega_0^2 = 2$, $F = \frac{1}{2}$, and with a source term $\boldsymbol{f}(\boldsymbol{x}, t)$ and $\boldsymbol{g}(\boldsymbol{x}, t)$ added to the right hand sides of (2.7) and (2.8), respectively. More specifically, the analytical solution is as follows:

$$
\boldsymbol{E}(\boldsymbol{x}, t) = \begin{pmatrix} E_x \\ E_y \\ E_z \end{pmatrix} = \begin{pmatrix} A\cos\pi x\sin\pi y\sin\pi z \\ B\sin\pi x\cos\pi y\sin\pi z \\ C\sin\pi x\sin\pi y\cos\pi z \end{pmatrix} e^{-t}\cos t,
$$

$$
\boldsymbol{H}(\boldsymbol{x}, t) = \begin{pmatrix} H_x \\ H_y \\ H_z \end{pmatrix} = \begin{pmatrix} \pi(C-B)\sin\pi x\cos\pi y\cos\pi z \\ \pi(A-C)\cos\pi x\sin\pi y\cos\pi z \\ \pi(B-A)\cos\pi x\cos\pi y\sin\pi z \end{pmatrix} e^{-t}\cos t,
$$

$$
\begin{aligned}
\boldsymbol{K}(\boldsymbol{x}, t) &= \begin{pmatrix} K_x \\ K_y \\ K_z \end{pmatrix}\\
&= \begin{pmatrix} \pi(C-B)\sin\pi x\cos\pi y\cos\pi z \\ \pi(A-C)\cos\pi x\sin\pi y\cos\pi z \\ \pi(B-A)\cos\pi x\cos\pi y\sin\pi z \end{pmatrix} e^{-t}\left[-\frac{1}{2}t\sin t + \frac{1}{2}\sin t + \frac{1}{2}t\cos t\right],
\end{aligned}
$$

$$
\boldsymbol{M}(\boldsymbol{x}, t) = \begin{pmatrix} M_x \\ M_y \\ M_z \end{pmatrix} = \begin{pmatrix} \pi(C-B)\sin\pi x\cos\pi y\cos\pi z \\ \pi(A-C)\cos\pi x\sin\pi y\cos\pi z \\ \pi(B-A)\cos\pi x\cos\pi y\sin\pi z \end{pmatrix} e^{-t}\cdot\frac{1}{2}t\sin t,
$$

$$\boldsymbol{J}(\boldsymbol{x},t)=\begin{pmatrix}J_x\\J_y\\J_z\end{pmatrix}=\begin{pmatrix}A\cos\pi x\sin\pi y\sin\pi z\\B\sin\pi x\cos\pi y\sin\pi z\\C\sin\pi x\sin\pi y\cos\pi z\end{pmatrix}e^{-t}\sin t,$$

where constants $A=1, B=2, C=-3$. It is easy to check that our constructed solutions satisfy the boundary conditions

$$\boldsymbol{n}\times\boldsymbol{E}=\boldsymbol{0}\quad\text{on }\partial\Omega,$$

and the Gauss's Law

$$\nabla\cdot\boldsymbol{E}(\boldsymbol{x},t)=0,\qquad\nabla\cdot\boldsymbol{H}(\boldsymbol{x},t)=0,\quad\forall(\boldsymbol{x},t)\in\Omega\times[0,1].$$

Furthermore, the source terms $\boldsymbol{f}$ and $\boldsymbol{g}$ are

$$\boldsymbol{f}(\boldsymbol{x},t)=\frac{\partial\boldsymbol{E}}{\partial t}-\nabla\times\boldsymbol{H}+\boldsymbol{J}=\begin{pmatrix}(-A-3A\pi^2)\cos\pi x\sin\pi y\sin\pi z\\(-B-3B\pi^2)\sin\pi x\cos\pi y\sin\pi z\\(-C-3C\pi^2)\sin\pi x\sin\pi y\cos\pi z\end{pmatrix}e^{-t}\cos t,$$

and

$$\begin{aligned}\boldsymbol{g}(\boldsymbol{x},t)&=\frac{\partial\boldsymbol{H}}{\partial t}+\nabla\times\boldsymbol{E}+\boldsymbol{K}\\&=\begin{pmatrix}\pi(C-B)\sin\pi x\cos\pi y\cos\pi z\\\pi(A-C)\cos\pi x\sin\pi y\cos\pi z\\\pi(B-A)\cos\pi x\cos\pi y\sin\pi z\end{pmatrix}e^{-t}\left[-\frac{1}{2}t\sin t-\frac{1}{2}\sin t+\frac{1}{2}t\cos t\right].\end{aligned}$$

In practical implementation of (3.20)–(3.23) with added source terms $\boldsymbol{f},\boldsymbol{g}$ and our assumed parameter values, the scheme can be implemented as follows: at each time step, we first solve $\boldsymbol{E}_h^k$ and $\boldsymbol{K}_h^k$ (can be done in parallel) from

$$\big(\boldsymbol{E}_h^k,\boldsymbol{\phi}_h\big)=\big(\boldsymbol{E}_h^{k-1},\boldsymbol{\phi}_h\big)+\tau\big[\big(\boldsymbol{H}_h^{k-\frac{1}{2}},\nabla\times\boldsymbol{\phi}_h\big)-\big(\boldsymbol{J}_h^{k-\frac{1}{2}},\boldsymbol{\phi}_h\big)+\big(\boldsymbol{f}^{k-\frac{1}{2}},\boldsymbol{\phi}_h\big)\big],\tag{4.1}$$

$$\big(\boldsymbol{K}_h^k,\tilde{\boldsymbol{\psi}}_{1h}\big)=\frac{1-\tau}{1+\tau}\big(\boldsymbol{K}_h^{k-1},\tilde{\boldsymbol{\psi}}_{1h}\big)+\frac{\tau}{1+\tau}\big[\big(\boldsymbol{H}_h^{k-\frac{1}{2}},\tilde{\boldsymbol{\psi}}_{1h}\big)-2\big(\boldsymbol{M}_h^{k-\frac{1}{2}},\tilde{\boldsymbol{\psi}}_{1h}\big)\big],\tag{4.2}$$

respectively; then solve $\boldsymbol{H}_h^{k+\frac{1}{2}},\boldsymbol{M}_h^{k+\frac{1}{2}},\boldsymbol{J}_h^{k+\frac{1}{2}}$ (can be done in parallel) from

$$\big(\boldsymbol{H}_h^{k+\frac{1}{2}},\boldsymbol{\psi}_h\big)=\big(\boldsymbol{H}_h^{k-\frac{1}{2}},\boldsymbol{\psi}_h\big)+\tau\big[\big(\boldsymbol{g}^k,\boldsymbol{\psi}_h\big)-\big(\nabla\times\boldsymbol{E}_h^k,\boldsymbol{\psi}_h\big)-\big(\boldsymbol{K}_h^k,\boldsymbol{\psi}_h\big)\big],\tag{4.3}$$

$$\big(\boldsymbol{M}_h^{k+\frac{1}{2}},\tilde{\boldsymbol{\psi}}_{2h}\big)=\big(\boldsymbol{M}_h^{k-\frac{1}{2}},\tilde{\boldsymbol{\psi}}_{2h}\big)+\tau\big(\boldsymbol{K}_h^k,\tilde{\boldsymbol{\psi}}_{2h}\big),\tag{4.4}$$

$$\big(\boldsymbol{J}_h^{k+\frac{1}{2}},\tilde{\boldsymbol{\phi}}_h\big)=\frac{1-\frac{\tau}{2}}{1+\frac{\tau}{2}}\big(\boldsymbol{J}_h^{k-\frac{1}{2}},\tilde{\boldsymbol{\phi}}_h\big)+\frac{\tau}{1+\frac{\tau}{2}}\big(\boldsymbol{E}_h^k,\tilde{\boldsymbol{\phi}}_h\big),\tag{4.5}$$

respectively.

Table 1 The L_2 errors obtained with fixed $\tau = 0.001$ on uniform cubic meshes

Mesh	$h = 1/4$	$h = 1/8$	Rate	$h = 1/16$	Rate	$h = 1/32$	Rate	$h = 1/64$	Rate
$\boldsymbol{E}$	0.07321974804515	0.03158144876304	1.2131	0.01512708431675	1.0619	0.00747996346401	1.0160	0.00372951942652	1.0040
$\boldsymbol{H}$	0.44956449669291	0.22803936788716	0.9792	0.11441369556450	0.9950	0.05725557574842	0.9987	0.02863386164873	0.9997
$\boldsymbol{K}$	0.22537864219636	0.11428171735782	0.9797	0.05734195107153	0.9949	0.02869618602232	0.9987	0.01435124721525	0.9997
$\boldsymbol{M}$	0.34923781635062	0.17729371835233	0.9780	0.08898779585895	0.9944	0.04453672505271	0.9986	0.02227372282081	0.9996
$\boldsymbol{J}$	0.09559775936104	0.04680869522871	1.0302	0.02325442822805	1.0092	0.01160754399864	1.0024	0.00580128323964	1.0006

Table 2 Total degrees of freedom (DOFs) on uniform cubic meshes and CPU time

Mesh	Total edge DOFs	Total face DOFs	CPU (in seconds)
$h = 1/4$	108	144	278.10
$h = 1/8$	1176	1344	418.14
$h = 1/16$	10800	11520	1456.92
$h = 1/32$	92256	95232	10044.55
$h = 1/64$	762048	774144	83435.97

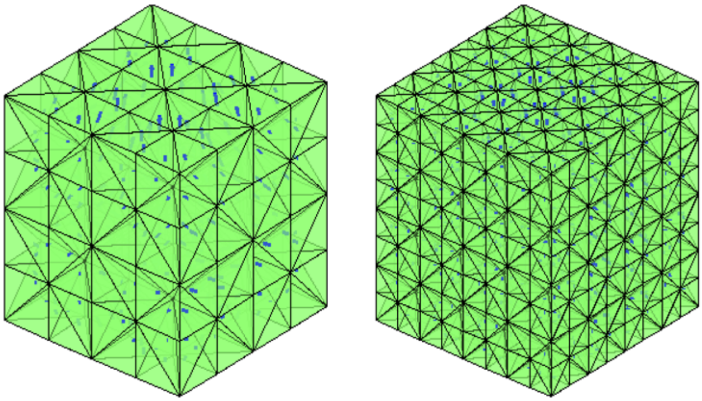

Fig. 1 Electric fields at $T = 1$ obtained on tetrahedral meshes: on $4 \times 4 \times 4$ mesh (*left*) and $8 \times 8 \times 8$ mesh (*right*)

We tested the algorithm (4.1)–(4.5) on both uniformly refined cubic and tetrahedral meshes with various time step size τ. Exemplary convergence results obtained with $\tau = 0.001$ are presented in Tables 1 and 3 for cubic and tetrahedral meshes, respectively. The results in both tables clearly show $O(h)$ convergence in the L_2 norm as our theoretical analysis proved in Theorem 3.4. The corresponding total degrees of freedom and CPU time are shown in Tables 2 and 4, from which we can see that our algorithm is quite efficient. Note that all our tests are carried out under MATLAB 7.0 running on a Dell desktop with 2 GB memory and 2.93 GHz CPU.

In Fig. 1 we presented the electric fields obtained with $\tau = 0.001$ on two different tetrahedral meshes. Since such 3D figures are not easy to see clearly, then we presented some slice cuts in Figs. 2 and 3 on the plane $z = 0.4$, i.e., we plotted the electric field (E_x, E_y) and (H_x, H_y) on $z = 0.4$.

5 Concluding Remarks

In this paper, we carried out the first mathematical study of another popular metamaterial model (we named it as the plasma-Lorentz model) used by physicists and engineers. Here we discussed the well-posedness of this model, developed two fully-discrete finite element methods for solving it, and proved the corresponding stability analysis and error estimates. Numerical results supporting our analysis are presented. More recently developed numerical schemes such as hp FEMs [10, 43] and DG methods [18], and practical applications of this model will be investigated in our future work.

Table 3 The L_2 errors obtained with fixed $\tau = 0.001$ on uniform tetrahedral meshes

Mesh	$h = 1/4$	$h = 1/8$	Rate	$h = 1/16$	Rate	$h = 1/32$	Rate
$\boldsymbol{E}$	0.092098770861475	0.045327653338625	1.0228	0.020277868881006	1.1605	0.01047714180926	0.9526
$\boldsymbol{H}$	0.504406698572890	0.255599924727033	0.9807	0.12836666877959	0.9936	0.06422141828145	0.9991
$\boldsymbol{K}$	0.246100548135429	0.125769396835022	0.9685	0.06322961398876	0.9921	0.03165805228652	0.9980
$\boldsymbol{M}$	0.377975552699024	0.193696304079489	0.9654	0.09745143062321	0.9910	0.04880159180433	0.9977
$\boldsymbol{J}$	0.124869622498626	0.062366916055371	1.0016	0.03113789242166	1.0021	0.01556400117940	1.0004

Table 4 Total degrees of freedom (DOFs) on uniform tetrahedral meshes and CPU time

Mesh	Total edge DOFs	Total face DOFs	CPU (in seconds)
$h = 1/4$	316	672	354.16
$h = 1/8$	3032	5760	1062.75
$h = 1/16$	26416	47616	7820.99
$h = 1/32$	220256	387072	71453.09

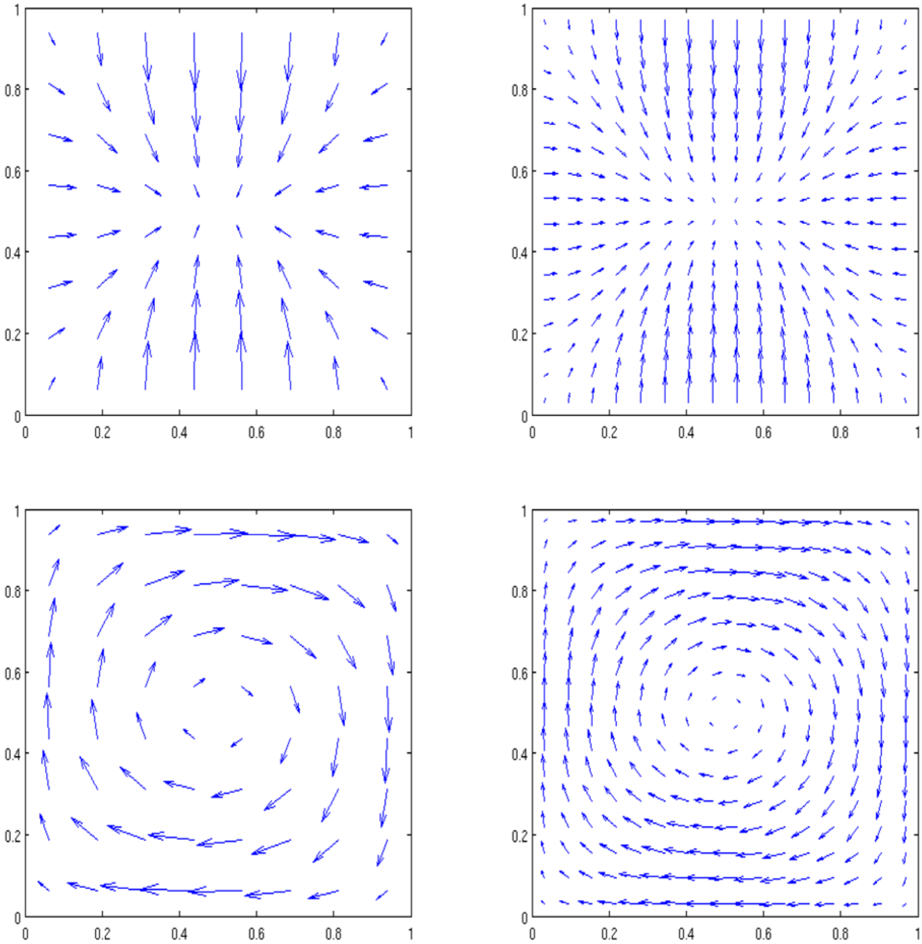

Fig. 2 Slice cuts at $T = 1$ obtained on cubic meshes: electric field (E_x, E_y) on 8×8 mesh (*top left*) and 16×16 mesh (*top right*); magnetic field (H_x, H_y) on 8×8 mesh (*bottom left*) and 16×16 mesh (*bottom right*)

Acknowledgements This work was supported by National Science Foundation grant DMS-0810896, and in part by the NSFC Key Project 11031006 and Hunan Provincial NSF project 10JJ7001.

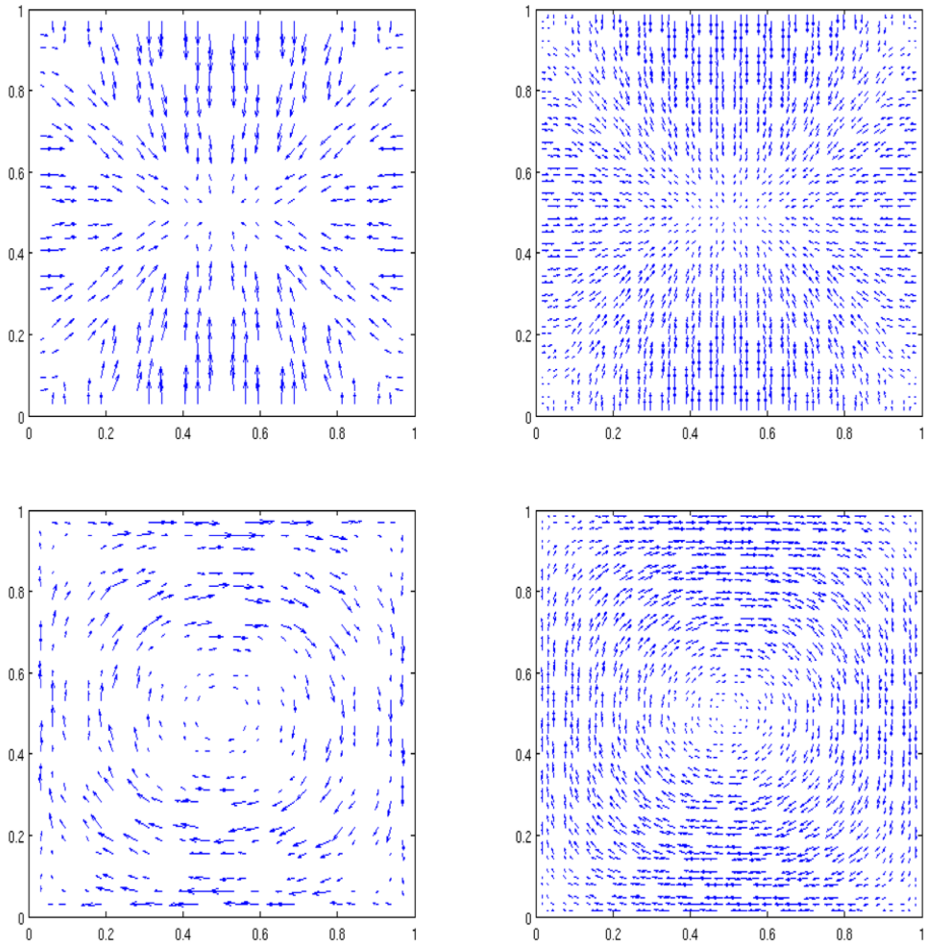

Fig. 3 Slice cuts at $T = 1$ obtained on tetrahedral meshes: electric field (E_x, E_y) on 8×8 mesh (*top left*) and 16×16 mesh (*top right*); magnetic field (H_x, H_y) on 8×8 mesh (*bottom left*) and 16×16 mesh (*bottom right*)

References

1. Banks, H.T., Bokil, V.A., Gibson, N.L.: Analysis of stability and dispersion in a finite element method for Debye and Lorentz media. Numer. Methods Partial Differ. Equ. **25**, 885–917 (2009)
2. Beck, R., Hiptmair, R., Hoppe, R.H.W., Wohlmuth, B.: Residual based a posteriori error estimators for eddy current computation. Modél. Math. Anal. Numér. **34**, 159–182 (2000)
3. Boardman, A.D., Marinov, K.: Electromagnetic energy in a dispersive metamaterial. Phys. Rev. B **73**, 165110 (2006)
4. Bochev, P.B., Garasi, C.J., Hu, J.J., Robinson, A.C., Tuminaro, R.S.: An improved algebraic multigrid method for solving Maxwell's equations. SIAM J. Sci. Comput. **25**, 623–642 (2003)
5. Bonnet-Ben Dhia, A.S., Ciarlet, P. Jr., Zwölf, C.M.: Time harmonic wave diffraction problems in materials with sign-shifting coefficients. J. Comput. Appl. Math. **234**, 1912–1919 (2010)
6. Chen, Z., Du, Q., Zou, J.: Finite element methods with matching and nonmatching meshes for Maxwell equations with discontinuous coefficients. SIAM J. Numer. Anal. **37**, 1542–1570 (2000)
7. Ciarlet, P. Jr., Zou, J.: Fully discrete finite element approaches for time-dependent Maxwell's equations. Numer. Math. **82**, 193–219 (1999)

8. Cockburn, B., Li, F., Shu, C.-W.: Locally divergence-free discontinuous Galerkin methods for the Maxwell equations. J. Comput. Phys. **194**, 588–610 (2004)
9. Cui, T.J., Smith, D.R., Liu, R. (eds.): Metamaterials: Theory, Design, and Applications. Springer, Berlin (2009)
10. Demkowicz, L., Kurtz, J., Pardo, D., Paszynski, M., Rachowicz, W., Zdunek, A.: Computing with hp-Adaptive Finite Elements. Vol. 2. Frontiers: Three Dimensional Elliptic and Maxwell Problems with Applications. CRC Press/Taylor & Francis, Boca Raton (2006)
11. Donderici, B., Teixeira, F.L.: Mixed finite-element time-domain method for Maxwell equations in doubly-dispersive media. IEEE Trans. Microw. Theory Tech. **56**, 113–120 (2008)
12. Engheta, N., Ziolkowski, R.W.: Electromagnetic Metamaterials: Physics and Engineering Explorations. Wiley-IEEE Press, New York (2006)
13. Fernandes, P., Raffetto, M.: Well posedness and finite element approximability of time-harmonic electromagnetic boundary value problems involving bianisotropic materials and metamaterials. Math. Models Methods Appl. Sci. **19**, 2299–2335 (2009)
14. Fezoui, L., Lanteri, S., Lohrengel, S., Piperno, S.: Convergence and stability of a discontinuous Galerkin time-domain method for the heterogeneous Maxwell equations on unstructured meshes. Math. Model. Numer. Anal. **39**, 1149C1176 (2005)
15. Frantzeskakis, D.J., Ioannidis, A., Roach, G.F., Stratis, I.G., Yannacopoulos, A.N.: On the error of the optical response approximation in chiral media. Appl. Anal. **82**, 839–856 (2003)
16. Gopalakrishnan, J., Pasciak, J.E., Demkowicz, L.F.: Analysis of a multigrid algorithm for time harmonic Maxwell equations. SIAM J. Numer. Anal. **42**, 90–108 (2004)
17. Hao, Y., Mittra, R.: FDTD Modeling of Metamaterials: Theory and Applications. Artech House, Boston (2008)
18. Hesthaven, J.S., Warburton, T.: Nodal Discontinuous Galerkin Methods: Algorithms, Analysis, and Applications. Springer, New York (2008)
19. Hiptmair, R.: Finite elements in computational electromagnetism. Acta Numer. **11**, 237–339 (2002)
20. Houston, P., Perugia, I., Schötzau, D.: Energy norm a posteriori error estimation for mixed discontinuous Galerkin approximations of the Maxwell operator. Comput. Methods Appl. Mech. Eng. **194**, 499–510 (2005)
21. Huang, Y., Li, J.: Recent advances in time-domain Maxwell's equations in metamaterials. In: Zhang, W., et al. (eds.) Lecture Notes in Computer Sciences, vol. 5938, pp. 48–57 (2010)
22. Hyman, J.M., Shashkov, M.: Mimetic discretizations for Maxwell's equations. J. Comput. Phys. **151**, 881–909 (1999)
23. Li, J.: Numerical convergence and physical fidelity analysis for Maxwell's equations in metamaterials. Comput. Methods Appl. Mech. Eng. **198**, 3161–3172 (2009)
24. Li, J.: Finite element study of the Lorentz model in metamaterials. Comput. Methods Appl. Mech. Eng. **200**, 626–637 (2011)
25. Li, J., Wood, A.: Finite element analysis for wave propagation in double negative metamaterials. J. Sci. Comput. **32**, 263–286 (2007)
26. Lu, T., Zhang, P., Cai, W.: Discontinuous Galerkin methods for dispersive and lossy Maxwell's equations and PML boundary conditions. J. Comput. Phys. **200**, 549–580 (2004)
27. Lin, Q., Yan, N.: Global superconvergence for Maxwell's equations. Math. Comput. **69**, 159–176 (1999)
28. Maradei, F., Ke, H., Hubing, T.H.: Full-wave model of frequency-dispersive media with Debye dispersion relation by circuit-oriented FEM. IEEE Trans. Electromagn. Compat. **51**, 312–319 (2009)
29. Markos, P., Soukoulis, C.M.: Wave Propagation: From Electrons to Photonic Crystals and Left-Handed Materials. Princeton University Press, Princeton (2008)
30. Monk, P.: Finite Element Methods for Maxwell's Equations. Oxford University Press, Oxford (2003)
31. Nédélec, J.-C.: Mixed finite elements in R^3. Numer. Math. **35**, 315–341 (1980)
32. Pendry, J.B.: Negative refraction makes a perfect lens. Phys. Rev. Lett. **85**, 3966–3969 (2000)
33. Pendry, J.B., Holden, A.J., Robbins, D.J., Stewart, W.J.: Magnetism from conductors and enhanced nonlinear phenomena. IEEE Trans. Microw. Theory Tech. **47**, 2075–2084 (1999)
34. Qiao, Z., Yao, C., Jia, S.: Superconvergence and extrapolation analysis of a nonconforming mixed finite element approximation for time-harmonic Maxwell's equations. J. Sci. Comput. **46**, 1–19 (2011)
35. Rieben, R.N., Rodrigue, G.H., White, D.A.: A high order mixed vector finite element method for solving the time dependent Maxwell equations on unstructured grids. J. Comput. Phys. **204**, 490–519 (2005)
36. Rodriguez-Esquerre, V.F., Koshiba, M., Hernandez-Figueroa, H.E.: Frequency-dependent envelope finite-element time-domain analysis of dispersion materials. Microw. Opt. Technol. Lett. **44**, 13–16 (2005)
37. Scheid, C., Lanteri, S.: Convergence of a discontinuous Galerkin scheme for the mixed time domain Maxwell's equations in dispersive media. INRIA preprint, No. 7364, May (2011)

38. Shaw, S.: Finite element approximation of Maxwell's equations with Debye memory, Advances in Numerical Analysis, Vol. 2010, Article ID 923832, 28 pp. (2010)
39. Shelby, R.A., Smith, D.R., Nemat-Nasser, S.C., Schultz, S.: Microwave transmission through a two-dimensional, isotropic, left-handed metamaterial. Appl. Phys. Lett. **78**(4), 489–491 (2001)
40. Shelby, R.A., Smith, D.R., Schultz, S.: Experimental verification of a negative index of refraction. Science **292**, 489–491 (2001)
41. Smith, D.R., Kroll, N.: Negative refractive index in left-handed materials. Phys. Rev. Lett. **85**, 2933–2936 (2000)
42. Smith, D.R., Padilla, W.J., Vier, D.C., Nemat-Nasser, S.C., Schultz, S.: Composite medium with simultaneously negative permeability and permittivity. Phys. Rev. Lett. **84**, 4184–4187 (2000)
43. Solin, P., Dubcova, L., Cerveny, J., Dolezel, I.: Adaptive hp-FEM with arbitrary-level hanging nodes for Maxwell's equations. Adv. Appl. Math. Mech. **2**, 518–532 (2010)
44. Stoykov, N.S., Kuiken, T.A., Lowery, M.M., Taflove, A.: Finite-element time-domain algorithms for modeling linear Debye and Lorentz dielectric dispersions at low frequencies. IEEE Trans. Biomed. Eng. **50**, 1100–1107 (2003)
45. Taflove, A., Hagness, S.C.: Computational Electrodynamics: The Finite-Difference Time-Domain Method. Artech House, Boston (2000)
46. Wang, B., Xie, Z., Zhang, Z.: Error analysis of a discontinuous Galerkin method for Maxwell equations in dispersive media. J. Comput. Phys. **229**, 8552–8563 (2010)